ACS OMEGA

http://pubs.acs.org/journal/acsodf

Article

Model Analysis for the Implementation of a Fast Model Predictive Control Scheme on the Absorption/Stripping CO_2 Capture Plants

Tahir Sultan, Haslinda Zabiri,* Muhammad Shahbaz, and Abdulhalim Shah Maulud

Cite This: *ACS Omega* 2022, 7, 8437−8455

Read Online

ACCESS | Metrics & More | Article Recommendations

ABSTRACT: The purpose of this paper is to investigate the possible implementation of the Fast model predictive control (MPC) scheme for chemical systems. Due to the difficulties associated with complicated dynamic behavior and model sensitivity, which results in considerable offsets, the Fast MPC controller has not been implemented on the CO_2 capture plant based on the absorption/stripping system. The main objective of this work is to evaluate the most appropriate model for implementing the Fast MPC control strategy, which results in fast output responses, negligible offsets, and minimum errors. The steady-state and dynamic simulation models of the CO_2 capture plant are designed in Aspen PLUS. In the System Identification Toolbox, multiple state-space models are identified to achieve a highly accurate model for the Fast MPC controller. The Fast MPC controller is then implemented to evaluate the performance under a setpoint tracking mode with ±5 and ±15% step changes. The results showed that the Fast MPC based on the state-space prediction focus model has on average 7.9 times lower offset than the simulation focus model and 10.4 times lower integral absolute error values. The comparison study concluded that the Fast MPC control strategy performs efficiently using prediction-based focus state-space models for CO_2 capture plants using the absorption/stripping system with minimum offsets and errors.

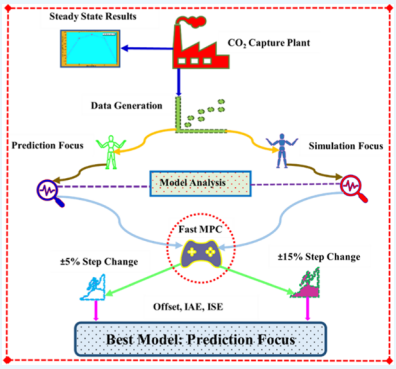

1. INTRODUCTION

Natural gas is a hydrocarbon gas mixture that mainly consists of methane. The gas from production wells commonly comprised hydrocarbons and impurities like carbon dioxide, hydrogen sulfide, nitrogen, water, and so forth.[1] These impurities decrease the natural gas quality, and equipment corrosion and fouling are the main drawbacks that affect the operational efficiency.[2] Due to high demand and usage, the utilization of wells having contaminated natural gas with CO_2 and H_2S is unavoidable.[3] Therefore, the design of low-cost and efficient CO_2 capture technologies is the utmost solution. Moreover, the greenhouse gases produced from fossil fuel-based power plants are the biggest source of climate change.[4] The main origin of CO_2 emission is fossil fuel-based power plants (coal and natural gas).[5] From this perspective, the carbon capture and storage technology is the crucial and essential alternative solution for smart and fast CO_2 capture to avoid equipment and environmental problems.[6,7]

Different carbon capture technologies have been designed like separation by hydrates, absorption, adsorption, distillation, membrane separation, chemical looping combustion, and biological separation.[8,9] Across all, amine-based absorption is the most feasible and commonly utilized technology for large-scale CO_2 absorption systems due to the advantages of easy retrofitting and high carbon capture efficiency.[10] However, amine-based absorption has also certain drawbacks like a high cost for the regeneration step in the stripping section, process nonlinearities, constraint limits, and variable interactions.[11] Therefore, developing an efficient, flexible, and fast responsive control strategy for such a system is critical either for natural gas treatment or reduction of CO_2 emissions in post-combustion processes.

In terms of advanced model-based control design, model predictive control (MPC) has been widely used to control the CO_2 capture systems effectively.[12−17] Rúa et al.[16] implemented the 5 × 5 (five MVs, five CVs) MPC control strategy on an natural gas combined-cycle (NGCC) plant. The standard MPC control strategy is also implemented on a CO_2 absorption/stripping system using MATLAB by Cormos et al.[12] Several step changes such as step, ramp, and sinusoidal are introduced into the inputs to control the CO_2 removal rate. The MPC controller has demonstrated superior performance in lowering the overshoot and regulating the limitations compared to a PI-based control scheme. He et al.[18] also proposed an MPC control structure for a CO_2 capture system in order to assess its controllability and flexibility. For load and

Received: October 26, 2021
Accepted: January 26, 2022
Published: February 28, 2022

https://doi.org/10.1021/acsomega.1c05974
ACS Omega 2022, 7, 8437−8455

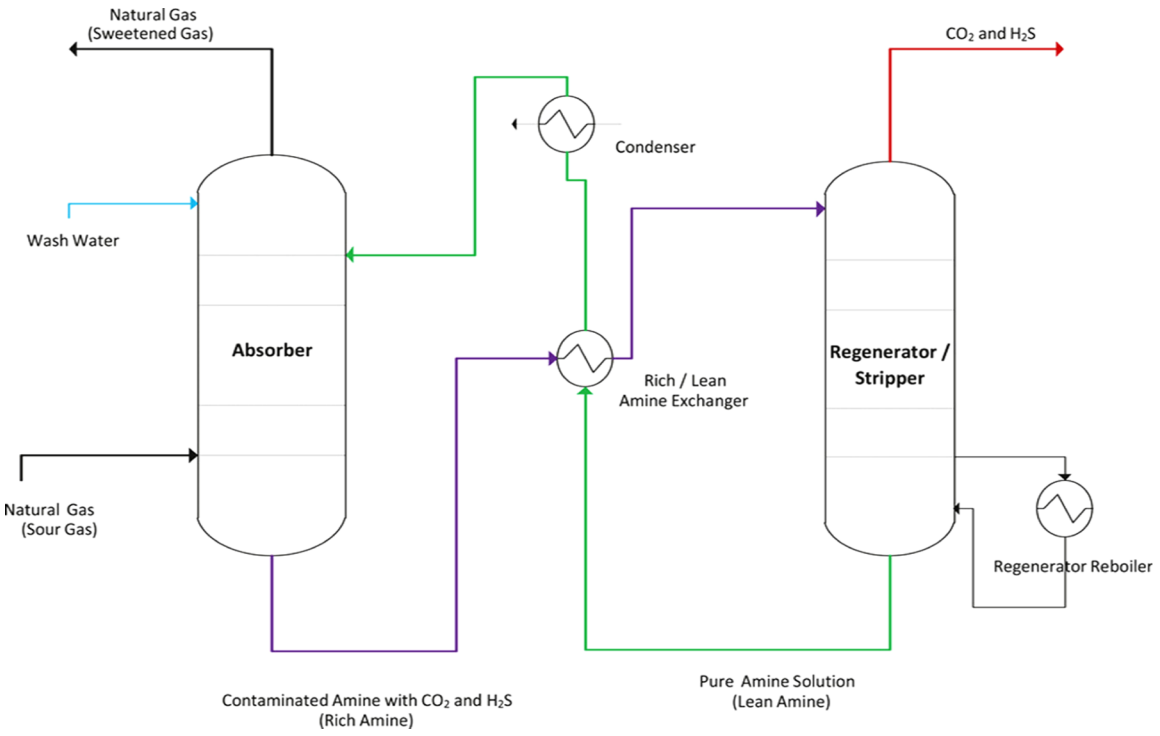

Figure 1. Basic process flow diagram for MEA-based absorption/stripping for acid gas removal from natural gas.[27]

setpoint tracking scenarios, the MPC controller's performance is evaluated by sudden changes. To address the demand for flexibility, Wu et al.[19] used an artificial neutral network and particle swarm optimization to develop an intelligent predictive controller to enhance the flexible operating performance of a large-scale CO_2 capture process.

Although nonlinear differential equations or nonlinear identification procedures are used to represent the dynamics of CO_2 capture systems properly, the nonlinearity distribution of CO_2 capture system over a wide range of conditions has not been quantified. For the design of a flexible control strategy, the distribution of nonlinearity and change of process dynamics over a wide range of operation circumstances might be difficult. Although the nonlinear MPC provides greater wide-range load variation, the nonlinear optimization process, which involves solving a large number of differential equations, is computationally inefficient and time intensive. Furthermore, developing an accurate nonlinear control model is challenging. However, a single linear controller can manage the capture system by selecting an appropriate control target and operating range. As a result, a linear MPC may be employed to efficiently regulate the CO_2 capture process according to the required operating conditions.[20]

The control algorithm of MPC is solved in the form of a quadratic program (QP). In standard or regular MPC, control action is calculated by solving an online optimization problem at each time step. The computational burden of the controller is increased due to the complex structure of QP, resulting in a delayed response time.[21] Furthermore, including constraints and variable interactions into the control algorithm (QP) results in a slower response. Alternatively, the computational burden of the MPC controller can be reduced by solving the QP fragmentally into small fractions and accelerating calculation time in control action utilizing online optimization called the Fast MPC approach.

The Fast MPC controller has been implemented widely on electrical or electronic systems, especially on robotic systems.[22−24] However, its implementation on the chemical process systems has not been reported so far. The Fast MPC controller is the ultimate solution for dealing with large settling times (slow output response). The Fast MPC controller exploits the QP into fragments, and the control action is solved fragmentally through online optimization. The concentration of CO_2 in the sweet gas is the most critical factor in ensuring that it always follows the appropriate setpoints in the event of a sudden disruption or change in setpoint. As a result, a fast-responding controller such as the Fast MPC may be beneficial, especially for post-combustion processes where various types of sudden input changes (step, ramp, and sinusoidal) may occur.

The Fast MPC controller is a model-sensitive controller as the computational (CPU) time and performance of any control strategy are largely dependent on the quality and structure of the identified model.[25] As a result, the model must be accurate enough to represent the real dynamics of the CO_2 capture process. However, the mathematical model should also be straightforward enough for the controller to complete the online computation promptly.

The purpose of this paper is to investigate the possible implementation of the Fast MPC controller scheme for chemical systems. Due to the difficulties associated with complicated dynamic behavior and model sensitivity, which results in considerable offsets, the Fast MPC controller has not been implemented on chemical systems. The main objective of this work is to evaluate the most appropriate model for implementing the Fast MPC control strategy, which results in fast output responses, negligible offsets, and minimum errors. In this paper, the suitable model for the Fast MPC control strategy implementation is evaluated using two prediction error minimization (PEM)-based method state-space models for the

https://doi.org/10.1021/acsomega.1c05974
ACS Omega 2022, 7, 8437−8455

absorption/stripping system of CO_2 capture plants. Based on the authors' knowledge, this is a novel study related to model comparison for the Fast MPC control scheme implementation on a CO_2 capture plant via an absorption/stripping system. In Aspen PLUS, a steady-state simulation model of the natural gas CO_2 capture plant is developed and then converted to a dynamic model for the generation of input−output data. Multiple state-space models (simulation/prediction focus) have been identified using the System Identification Toolbox in MATLAB using the generated input−output data. The controller performance is assessed in terms of settling time, offsets, CPU time, integral absolute error (IAE), and integral square error (ISE) for both models under step changes in the CO_2 composition and stripper temperature scenarios.

2. METHODOLOGY

2.1. Model Development. *2.1.1. Process Description.* The absorption/stripping process primarily comprises an absorber and a stripper as well as mixers, splitters, and a heat exchanger. The natural gas containing CO_2 enters from the bottom of the absorber where CO_2 is absorbed in the monoethanolamine (MEA) solvent flowing down in the absorber. The CO_2-rich solvent stream is delivered to the heat exchanger after absorption, where the temperature is increased to 100 °C. Furthermore, this rich solvent stream is sent to the stripper column for CO_2 separation and MEA solvent recovery. The CO_2 is absorbed in the MEA solvent through a weak chemical reaction. Therefore, to reverse that weak reaction, a high temperature is required in the stripper. A reboiler is used to maintain the high temperature around 105−110 °C inside the stripper as the higher temperature can degrade the MEA solvent.[26] The CO_2 gas is separated from the top of a stripper, while the regenerated MEA solvent as a lean solvent stream is sent back to the absorber through a heat exchanger, where the required temperature is achieved. The qualitative process flow diagram for the absorption/stripping system for natural gas processing has been shown in Figure 1.[27] In this work, the absorber column is designed on the basis of a CO_2 capture plant used for high pressure established in Universiti Teknologi PETRONAS (UTP), Malaysia.[28] A theoretical stripper has been added to this plant for the complete design of the absorption/stripping system. This theoretical stripper is designed based on the conventional design, as described in the literature.[28−31] The adequate contact area for CO_2 gas and MEA solvent inside the column is provided by structured or random packing. MacDowell et al.[32] proposed that the most promising option for carbon capture is structured packing because of its economical accessibility, large contact area, and low pressure drop. Therefore, the structured packing is utilized for the process design of the absorber column.

2.1.2. Steady-State Model. Aspen PLUS V.10 is utilized to design the simulation model of the absorption/stripping plant in the steady-state environment. The design incorporates a RadFrac absorber and stripper columns, as well as a heat exchanger, two mixers, a splitter, and numerous valves. The absorber column model is simulated based on the nominal conditions used in the UTP pilot plant.[28] The data for the feed stream and other streams are based on the UTP pilot plant, as reported in the work of Salvinder et al.[28] The operating conditions of all streams for both columns are listed in Table 1.

The heuristic approach is employed to calculate the height and diameter of the theoretical stripper on mass balance basis.[33] Additionally, a splitter is added to purge the extra lean solvent flow rate for the mass balance consistency of the model due to the cyclic nature of the simulation model. The stripper column is supposed to be cylindrical having a residence time of 10 min for the evaluation of design parameters. The stripper is designed to operate at 1.0 bar pressure with a total number of seven stages, which is less than the pressure of the absorber column of 10.32 bar. The higher pressure in the stripper requires high temperature for stripping, which can affect the MEA regeneration efficiency due to the thermal degradation of the solvent at high temperature.[26] A reboiler inside the stripper plays a key role in providing the heat for the regeneration step, and the reboiler heat duty is one of the challenging aspects in CO_2 capture plants based on the absorption/stripping system. Figure 2 illustrates the flowsheet of the steady-state simulation model designed in the Aspen PLUS steady-state environment. For steady-state tests, the flowrate and composition of the feed gas varied to monitor the CO_2 capture rate.

Table 1. Operating Parameters for the Steady-State Simulation of an Absorber and Stripper

operating conditions	sour gas	lean solvent	rich solvent
CO_2 (mole fraction)	0.5	0	0.10
CH_4 (mole fraction)	0.5	0	0.02
H_2O (moles fraction)	0	0.8	0.77
MEA (mole fraction)	0	0.2	0.11
temperature (°C)	25	25	100
pressure (bar)	10.6	10.5	1.05
flowrate (L/min)	50	1.1	1.82

To check the validity and correctness of the steady-state simulation model, the CO_2 capture rate of the designed simulation model is compared with the experimental data. As the current simulation model is designed based on the UTP pilot plant, the designed simulation model must achieve the CO_2 removal rate of 85% according to the experimental results.[28] The current simulation model is designed using an equilibrium-based modeling approach, and the model is adjusted by changing specific input conditions to achieve the CO_2 removal rate of approximately 85%. The final performance is illustrated in Table 2.

2.1.3. Dynamic Simulation Model. When the steady-state simulation model has successfully converged in Aspen PLUS, the model is then converted into the dynamic state in Aspen Dynamics. The pressure drop along all the necessary streams and equipment can be achieved by installing control valves or pumps. Moreover, the absorber and stripper are properly sized in the steady-state simulation model based on the UTP pilot plant and literature data, respectively. Although the rate-based modeling approach has higher accuracy than the equilibrium-based technique, Aspen Dynamics does not cater for the more complex rate-based models since the model may fail to converge. Hence equilibrium-based models are adopted for the dynamic analysis, and additional tuning is required in terms of the column efficiency and pressure drop. The modifications are necessary to account for the variation in CO_2 capture rates between the rate-based and equilibrium-based modeling approaches. The absorber/stripper stage numbers and the lean solvent flowrate are modified to reflect the rate-based modeling approach used by He et al.[31]

2.2. Input−Output Data Generation through PRBS. There are multiple variables available in the CO_2 capture plant based on the absorption/stripping system, which can be

https://doi.org/10.1021/acsomega.1c05974
ACS Omega 2022, 7, 8437−8455

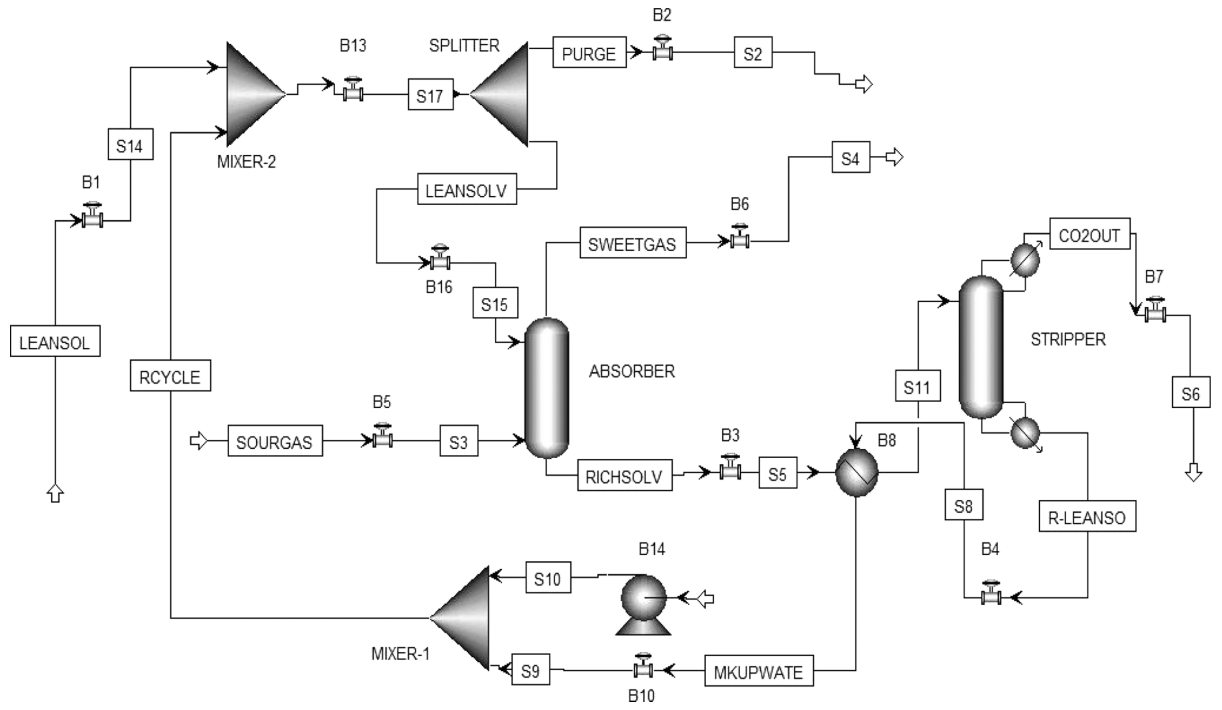

Figure 2. Steady-state simulation model of a CO_2 capture plant designed in Aspen PLUS.

Table 2. CO_2 Removal Rate Results of the UTP Pilot Plant and the Current Designed Steady-State Simulation Model

plant type	CO_2 removal rate (%)	modeling approach
experimental (UTP pilot plant)	85	rate-based
current simulation model	89.70	equilibrium-based

selected as input/manipulated variables (MVs) or output/control variables (CVs). The CO_2 composition in sweet gas is a strong indicator of CO_2 absorption in the lean solvent inside the absorber column. The less CO_2 concentration in the sweet gas results in more amount of CO_2 being absorbed in the lean solvent. It can be controlled through the amount of lean solvent available for absorption, which is associated with the lean solvent valve opening. The less regeneration or stripper energy requirement is the most challenging aspect of CO_2 capture systems as the solvent needs to be recovered in a cyclic process through the application of high temperature. Therefore, the temperature at the bottom of the stripper must be controlled accurately through the reboiler heat duty. The current study is based on a 2 × 2 system having two MVs; lean solvent valve opening (U_1) and reboiler heat duty (U_2), while the CO_2 composition in the sweet gas (Y_1) and stripper bottom temperature (Y_2) are the corresponding CVs.[34]

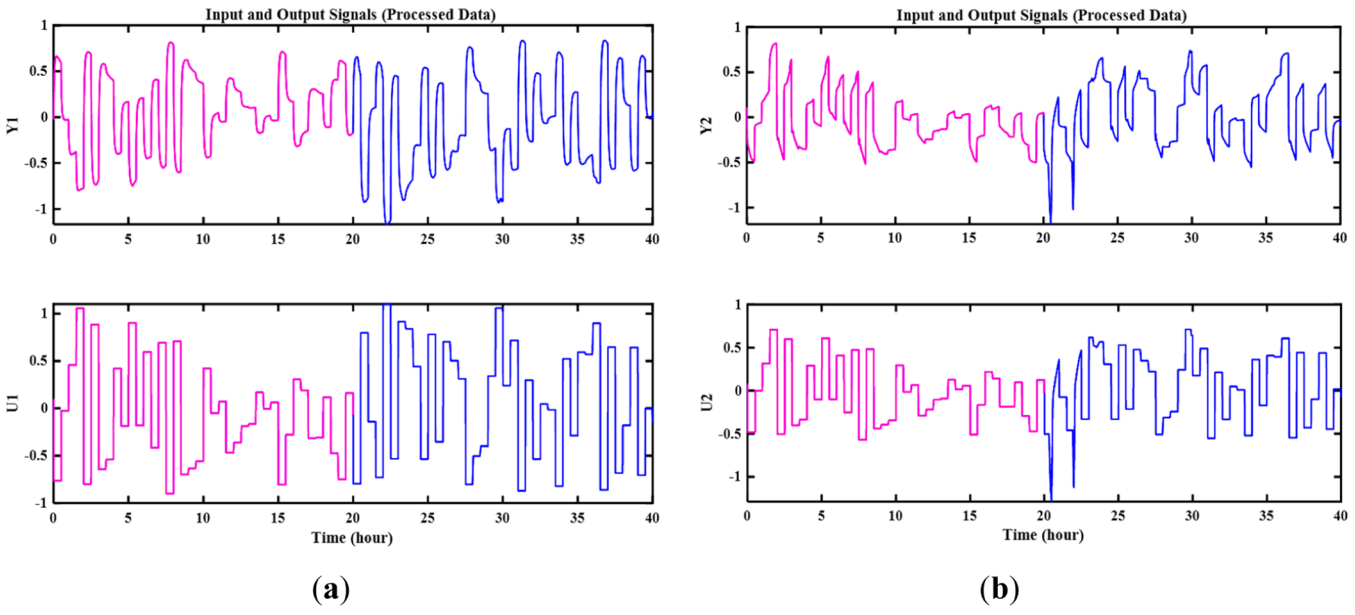

Figure 3. Pre-processed input−output produced from the dynamic model designed in Aspen Dynamics (a) Y_1 and U_1 and (b) Y_2 and U_2.

https://doi.org/10.1021/acsomega.1c05974
ACS Omega 2022, 7, 8437−8455

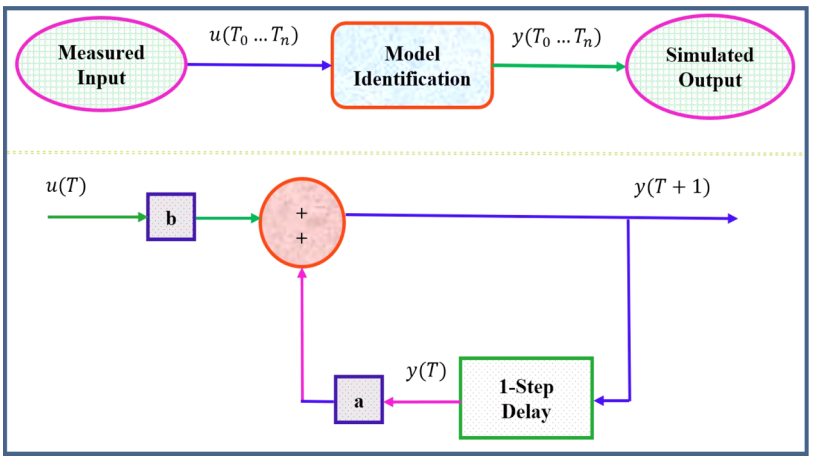

Figure 4. Mathematical calculation mechanism for the simulation focus model.

The data generation is an important step for system identification as the accuracy of the identified model is affected by the details supplied by the input−output data.[35] Using the developed Aspen Dynamics model designed in Section 2.2, the corresponding input−output data are generated by utilizing pseudorandom binary sequence (PRBS) signals by fixing the ±5% amplitude with respect to the datum point with a period of 30 min for U_1 and U_2. The design of the PRBS signals is a critical step that gathers the critical characteristics of the CO_2 capture plant by considering the plant outputs based on input changes.[30]

2.3. System Identification of the Mathematical Models. The real system, or dynamic simulation model, used in this study is a dynamically complicated system that necessitates a data-driven modeling method in order to establish a highly accurate model.[33] The generated input−output data having 4000 data points are then exported to MATLAB for data processing and model identification. The accuracy of the data-driven mathematical models depends heavily on the scaling of data utilized for system identification. Therefore, the data are processed by removing means and scaled (range of −1 to 1) to ensure that the identification process should consider all the data equally through minimizing the range difference of data signals.[35] Furthermore, the data are divided into two sets, each set having 2000 data points, which are used as working or training data and validation data. The pre-processed data for Y_1, U_1 and Y_2, U_2 are illustrated in Figure 3a,b, respectively.

For the controller implementation, two types of models have been identified: state-space based on simulation and prediction focus. The primary distinction between the state-space model based on prediction and the simulation focus is the distinctive identification procedure utilized in the System Identification Toolbox. The simulation focus approach identifies the model based on the input data and initial conditions. In prediction focus, the model response is computed at a specific time in the future using the current and prior values of the observable input, output values, and initial conditions.[36] The models are identified by utilizing the System Identification Toolbox in MATLAB.[37] The main steps for the system identification are as follows:

1. Data processing by removing the means and scaling the data through the range, as described earlier
2. The input−output data are imported in the System Identification Toolbox having starting time and sampling time of 0 and 0.01 h, respectively.
3. The data are divided into two data sets through the range, each having 2000 data points, which will be used as working and validation data.
4. The type of the mathematical model is selected such as transfer function models, state-space models, polynomial models, and so forth. The models selected in this study are the state-space model, as described earlier.
5. The model order value is chosen, and the order of the models in this study are 1st and 2nd.
6. The estimation method is picked in "estimation options" such as subspace (N4SID) and PEM. The PEM estimation method has been utilized in this work due to the advantages of high accuracy.
7. The focus type is selected to be either simulation or prediction from the "focus" option.
8. The search method is chosen from iteration options. In the "Options for Iterative Minimization" window, the search method is selected such as Gauss−Newton, trust-region reflective Newton (lsqnonlin), gradient search (grad), and so forth.
9. All the search methods are applied, and the models are estimated having the best fitting percentage for Y_1 and Y_2.
10. The same procedure is repeated for both types of state-space models (prediction and simulation focus), and the models having the best fitting percentage for both cases are found.

In the simulation focus model, the total sampling time of the model is equal to the sampling time of the input data used for dynamic simulation. It is supposed that a system having a single input (u) and a single output (y) with the total time T_n and the simulation focus model will generate a model with the output $y(T_0 \ldots T_n)$ based on the input $u(T_0 \ldots T_n)$. The simulation focus model will be calculated with 1-step delay, which will be equivalent to the total sampling time of the input used for dynamic simulation. The mechanism is shown in Figure 4.

In the prediction focus model, the output is projected K steps ahead of the measured input and output, where K is a prediction horizon corresponding to the predicted output at any time KT_s, and T_s is the sampling time. A dynamic system is assumed with the measured input $u_m(T_1 \ldots T_N)$ and a single

https://doi.org/10.1021/acsomega.1c05974
ACS Omega 2022, 7, 8437−8455

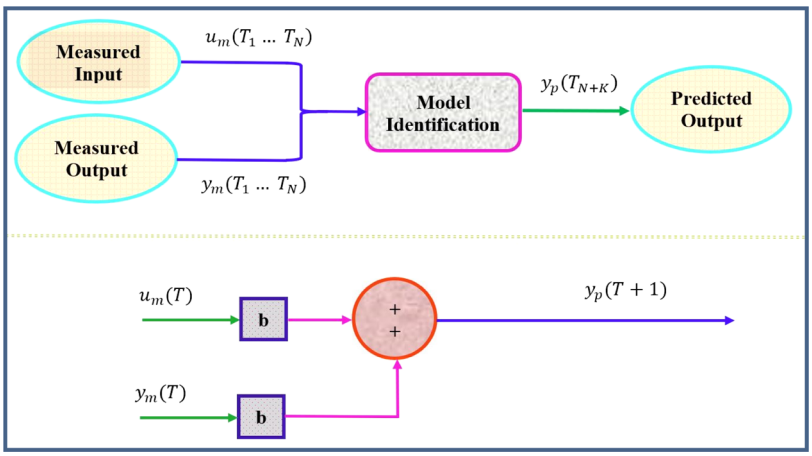

Figure 5. Mathematical calculation mechanism for the prediction focus model.

output $y_m(T_1 \dots T_N)$ having total sampling time of T_N, in which the prediction focus predicts the output response as $y_p(T_{N+K})$. The mathematical formulation is shown in Figure 5.

The general equations for the state-space model are shown in eqs 1 and 2, where A, B, C, and D are the system matrices for the state, input, output, and transmission, respectively, while $u(t)$ and $y(t)$ are input and output variables, and $\dot{x}(t)$ is a state variable.

$$\dot{x}(t) = Ax(t) + Bu(t) \tag{1}$$

$$y(t) = Cx(t) + Du(t) \tag{2}$$

There are multiple estimation methods for system identification in the Toolbox such as subspace (N4SID), PEM, and regularized reduction. The estimation method used in this work is the PEM method due to its high accuracy and fast estimation.[38] Several state-space models are identified based on different iteration search methods (adaptive Gauss−Newton, Levenberg−Marquardt, gradient search, trust-region reflective Newton, etc.) for both cases of simulation and prediction focus. The models having the best fitting percentage for both cases are used for Fast MPC controller implementation.

2.4. Fast MPC Controller Implementation. In the current work, the Fast MPC controller is implemented in the form of a MATLAB code file provided by Wang et al.[39] It is supposed that a linear dynamic model, as described in eqs 3 and 4, is used for MPC implementation, where x_{t+1}, u_t, and y_{t+1} are state, input, and output vectors, respectively, while A, B, and C are state, input, and output matrices, respectively.

$$x_{t+1} = Ax_t + Bu_t, \quad t = 0,1,2 \dots \tag{3}$$

$$y_{t+1} = Cx_{t+1} \tag{4}$$

The objective function or the generalized formulation of the Fast MPC for the above linear model is represented in eq 5, where Q, R, and T are the state weight matrix, input weight matrix, and prediction/planning horizon, respectively.[39] The control action is solved purely based on the prediction of states; the desired outputs or the setpoints are achieved through the optimization of states. The Fast MPC controller can deal with constraints effectively. Hence, eq 6 represents the upper and lower bound limits for states, inputs, and input changes.

$$\text{minimize} \rightarrow (x_{t+T})^T Q\,(x_{t+T}) + \sum_{t=0}^{t+T-1} (x_t)^T Q x_t + (\Delta u_t)^T R \Delta u_t \tag{5}$$

$$\begin{bmatrix} x_{\min} \le x_t \le x_{\max}, \\ u_{\min} \le u_t \le u_{\max}, \\ \Delta u_{\min} \le \Delta u_t \le \Delta u_{\max} \end{bmatrix} \tag{6}$$

The Fast MPC is software package in the form of a MATLAB code file, which further exploits the QP mentioned in eq 5 and solves the control problem fragmentally through online optimization purely based on system states.[39] There are two basic functions in the coding file to exploit the QP: "*fmpc_sim*" and "*fmpc_step*." The "*fmpc_step*" function solves the QP and optimizes the best state (x) and input (u) variables based on the step changes. The "*fmpc_sim*" function uses the calculated input and state values from the previous step to update the future best outputs for "t = 1,2,3...,*n*steps" according to the dynamics of the model. The control and state paths are initialized through previous values to generate the new inputs $(\tilde{u})$ and states $(\tilde{x})$ as follows

$$\tilde{u} = Kx(T), \quad \tilde{x} = Ax(T) + BKx(T) \tag{7}$$

Here, K is the gain matrix or the control gain, which is calculated based on pole locations. K is represented in eq 8 in terms of input weight (R), output/state weight (Q), state (A), and input (B) matrix. As the control actions in Fast MPC is solved through the gain matrix based on the states and pole locations, the offset removal term is missing in the corresponding mathematical equations of the control algorithm. Therefore, offsets are reduced to negligible levels through the optimization of key tunning parameters involved in Fast MPC, as mentioned in Table 3.

$$K = -(R + B^T Q B)^{-1} B^T Q A \tag{8}$$

The Fast MPC determines the optimal control actions for the real plant to achieve the desired setpoints. The control structure of the Fast MPC controller is based on the identified model, the observer, and the dynamic model. The observer is designed based on the identified model and the suitable pole locations. The plant outputs are measured based on the step changes, then the observer estimates the current states using the measured output along with inputs. The control structure

https://doi.org/10.1021/acsomega.1c05974
ACS Omega 2022, 7, 8437−8455

Table 3. Tuning Parameters Selected for Fast MPC

parameters	value
Q matrix	diag ([1 1)] variable
R matrix	diag ([1 1)] variable
pole locations	−0.52, −0.55
input constraints	$-10 \le u \le 10$
state constraints	$-20{,}000 \le x \le 20{,}000$
prediction horizon	50
control horizon	50
sampling time	0.01
barrier parameter K	0.01
iteration limit K^{max}	10
controller simulation time	200

for the Fast MPC with observer has been illustrated in Figure 6.

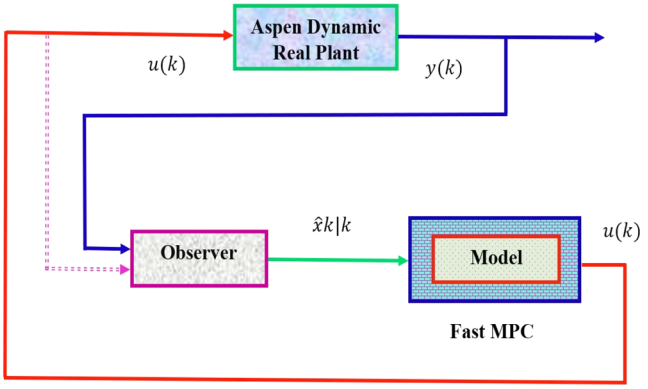

Figure 6. Process flow diagram of the control structure run in MATLAB.

Furthermore, values of different tuning parameters as barrier parameter k and iteration limit K^{max} are selected as 0.01 and 10, respectively, based on the work of Wang.[39] The values of all other tuning parameters for the implementation of Fast MPC using appropriate identified models are highlighted in Table 3.

The performance of the resulting Fast MPC controllers is evaluated under step changes of ±5 and ±15% introduced in the setpoints of both Y_1 and Y_2, respectively. The responses of U_1, U_2, Y_1, and Y_2 are observed, and the settling time, offset, CPU time, and errors (IAE and ISE) are calculated in terms of Y_1 and Y_2. The errors calculation especially the ISE value is one of the major aspects of the controller performance assessment.[13,40]

3. RESULTS AND DISCUSSION

3.1. Steady-State Results. The temperature profile along the stages of the absorber is shown in Figure 7a. The maximum amount of CO_2 gas is absorbed in the MEA-solvent through exothermic reactions having weak chemical bonds, while the overall temperature of the absorber is increased due to the exothermic reactions involved in CO_2 absorption. The rate of the reaction is maximum at the middle of the absorber; hence, the temperature is also maximum. Similarly, the stripper column has seven stages, and the CO_2-rich stream called the "S11" stream is introduced at stage 2 at 100 °C. The stripping or regeneration of MEA solvent is an energy-intensive process; hence, a high amount of heat is required to reverse the reactions, which stripped off the CO_2 and regenerate the MEA solvent for the next cycle.[41] The high energy requirement is fulfilled through the increase in S11 stream temperature and reboiler at the bottom of the stripper.[17] The heat duty of the reboiler is set based on the temperature requirement and CO_2 capture rate. A condenser is also installed at the top of the stripper to separate the water vapors from the segregated CO_2 stream. Therefore, the temperature at stage 1 is just around 27.15 °C for the effective condensation. The main stripping reactions take place at the bottom of the absorber due to the feasible temperature, which is required to break the weak chemical bonds. The temperature along the stripper stages is illustrated in Figure 7b.

3.2. Model Identification. Black-box models are purely data-driven models that are based on input−output data measurements. The quality of black-box models is highly dependent on the volume and quality of data.[42] There are different black-box models available in the System Identi-

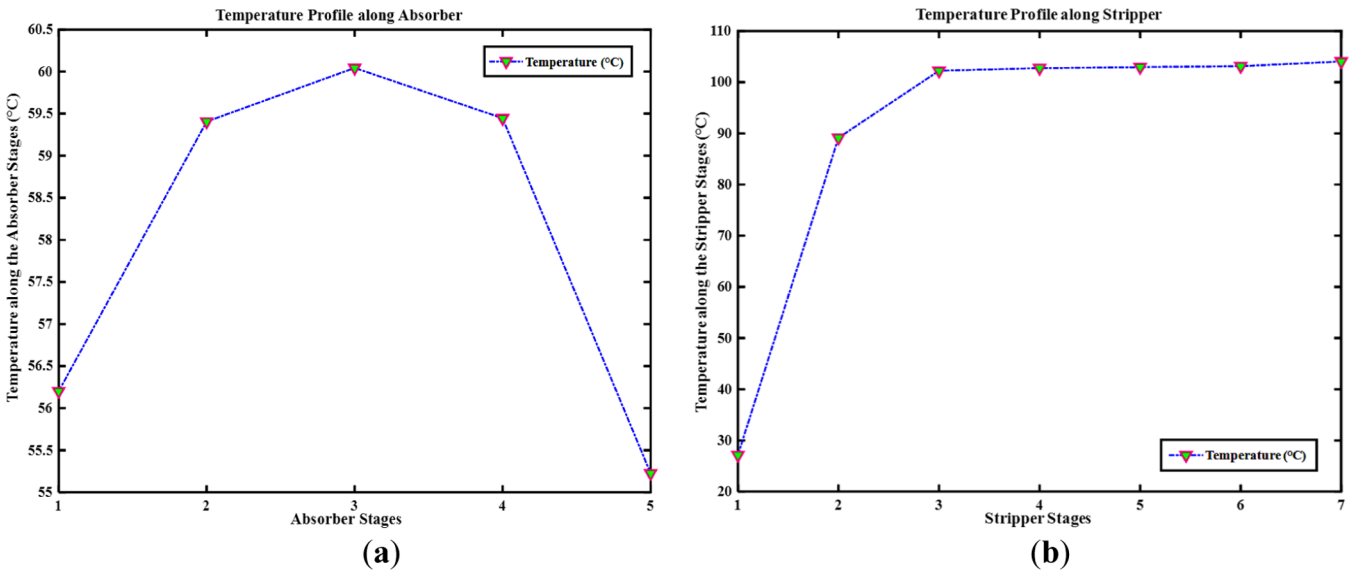

Figure 7. Steady-state model temperature profiles along the stages, (a) absorber and (b) stripper.

https://doi.org/10.1021/acsomega.1c05974
ACS Omega 2022, 7, 8437−8455

Table 4. Identified State-Space Models for Fast MPC Controller Implementation

			fitting %			
name	model type	order	Y_1 (%)	Y_2 (%)	focus	iteration search method
SS 1	state-space	1st	75.15	22.39	prediction	adaptive Gauss−Newton (gna)
SS 2	state-space	1st	83.32	58.62	prediction	trust-region reflective Newton (lsqnonlin)
SS 3	state-space	2nd	**92.33**	**84.80**	**prediction**	**trust-region reflective Newton** (lsqnonlin)
SS 4	state-space	1st	77.74	21.93	simulation	adaptive Gauss−Newton (gna)
SS 5	state-space	1st	84.34	57.57	simulation	trust-region reflective Newton (lsqnonlin)
SS 6	state-space	2nd	**88.17**	**75.74**	**simulation**	**trust-region reflective Newton (lsqnonlin)**

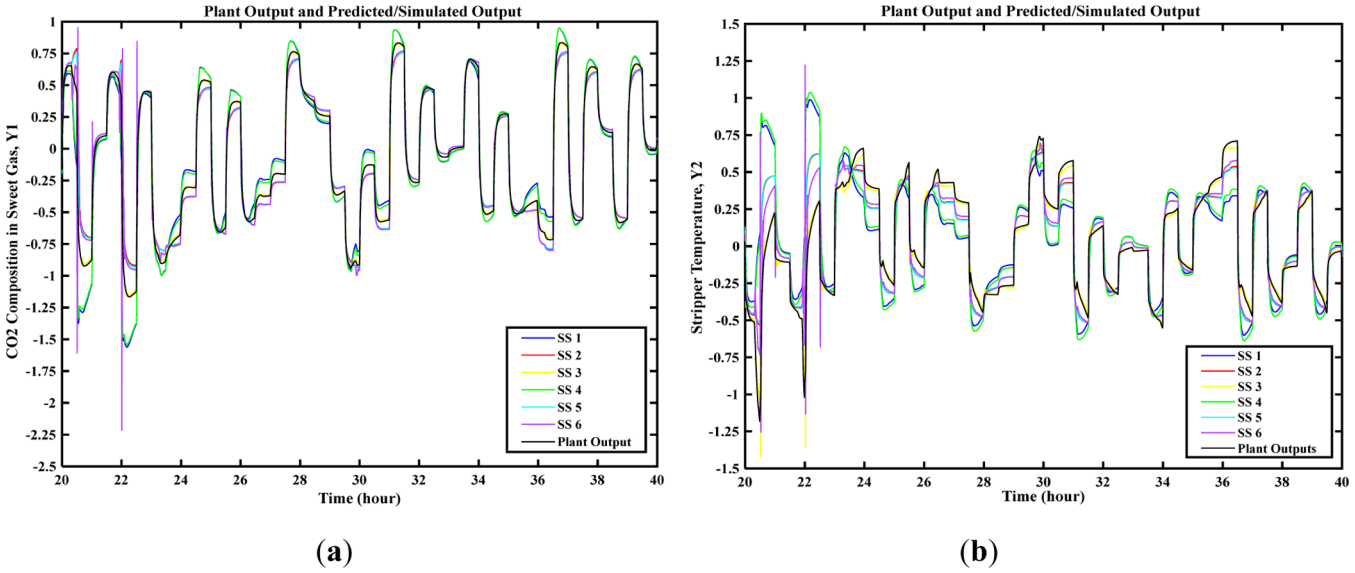

Figure 8. System identification results for state-space models: predicted/simulated vs plant outputs (a) Y_1 and (b) Y_2.

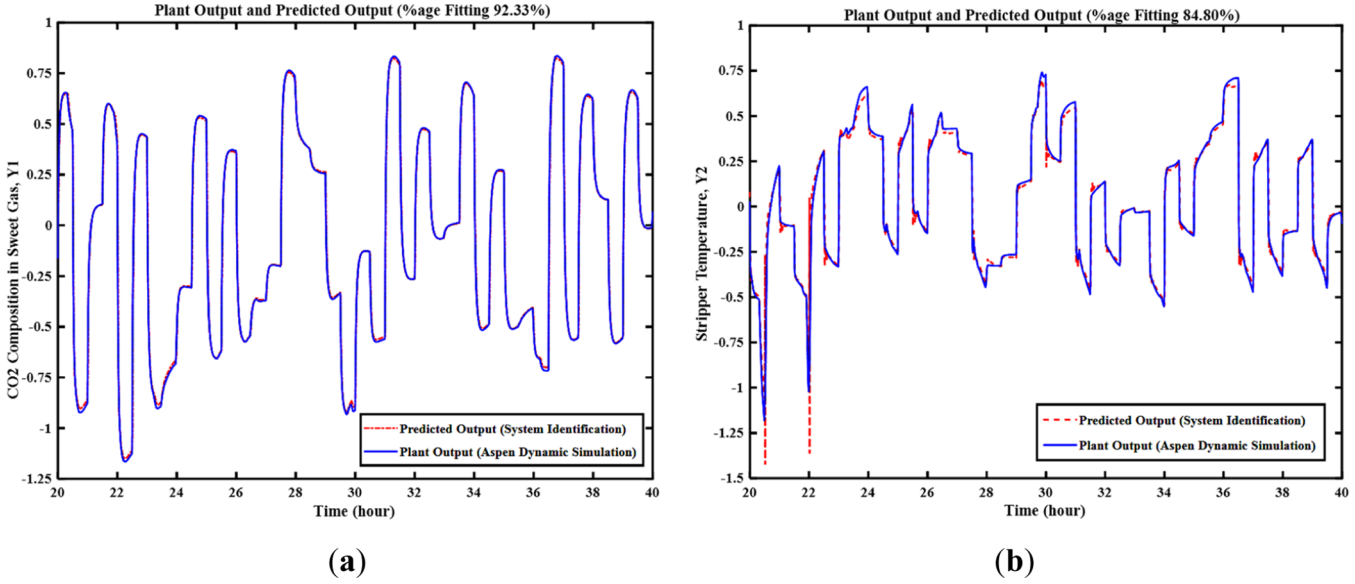

Figure 9. System identification results for model 1: predicted vs plant outputs (a) Y_1 and (b) Y_2.

fication Toolbox such as state space, transfer function, auto-regressive exogenous model, and so forth.[43] The data-driven approaches for system identification considering software packages such as CONTSID toolbox and open-source System Identification Package in Python can also be used for model identification based on the system requirement.[44−46] In this study, multiple state-space models are evaluated to achieve a model with high accuracy using the system identification approach and investigated for the implementation of the Fast MPC control scheme.

3.2.1. State-Space Models. To effectively represent the dynamics of a CO_2 capture system, the identified model must be sufficiently rigorous and precise. State-space models are regarded to be the ideal choice for controller implementations

https://doi.org/10.1021/acsomega.1c05974
ACS Omega 2022, 7, 8437−8455

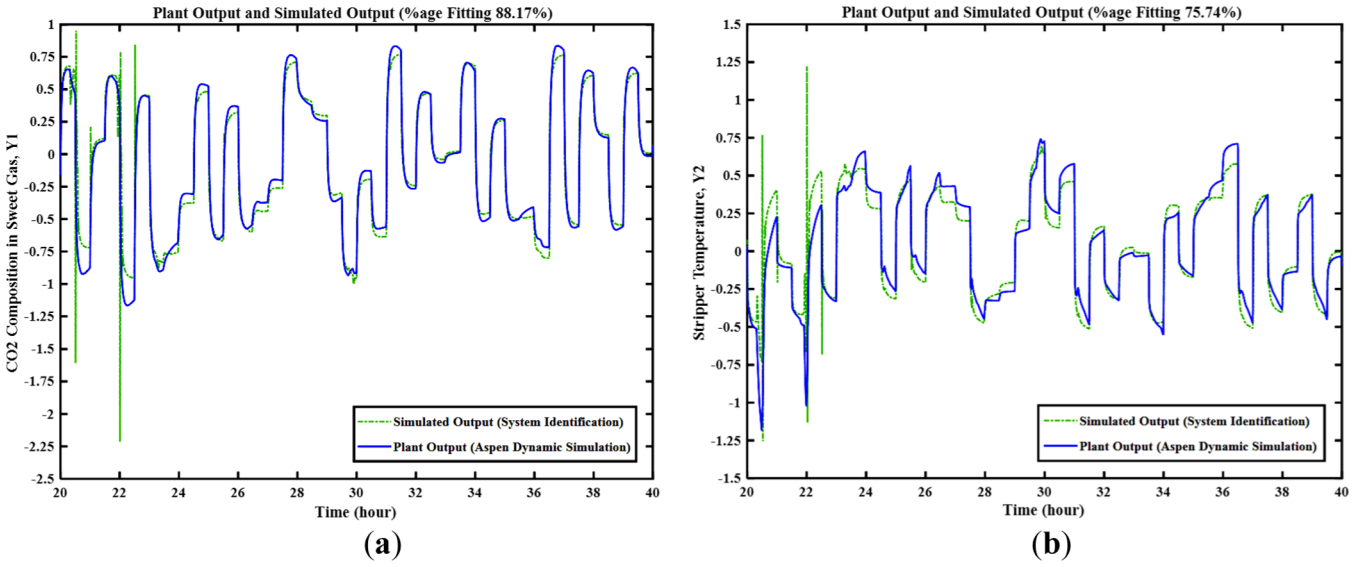

Figure 10. System identification results for model 2: simulated vs plant outputs (a) Y_1 and (b) Y_2.

Table 5. State-Space Equations for Identified Prediction and Simulation-Based Focus Models with *A*, *B*, *C*, and *D* Values

general equation of state-space model representation

$$\dot{x}(t) = Ax(t) + Bu(t) \quad (9)$$

$$y(t) = Cx(t) + Du(t) \quad (10)$$

state space equations for models 1 and 2

model 1

$$\begin{bmatrix}\dot{x}_1\\ \dot{x}_2\end{bmatrix} = \begin{bmatrix}-39.18 & -38.8\\ -29.12 & -33.41\end{bmatrix}\begin{bmatrix}x_1\\ x_2\end{bmatrix} + \begin{bmatrix}-3.686 & -0.1669\\ -3.825 & 1.826\end{bmatrix}\begin{bmatrix}u_1\\ u_2\end{bmatrix}$$

$$\begin{bmatrix}y_1\\ y_2\end{bmatrix} = \begin{bmatrix}6.755 & 2.924\\ -8.494 & -14.71\end{bmatrix}\begin{bmatrix}x_1\\ x_2\end{bmatrix} + \begin{bmatrix}0 & 0\\ 0 & 0\end{bmatrix}\begin{bmatrix}u_1\\ u_2\end{bmatrix}$$

model 2

$$\begin{bmatrix}\dot{x}_1\\ \dot{x}_2\end{bmatrix} = \begin{bmatrix}-43.29 & 16.47\\ 61.04 & -43.61\end{bmatrix}\begin{bmatrix}x_1\\ x_2\end{bmatrix} + \begin{bmatrix}-142.8 & 189.6\\ 476.1 & -683.6\end{bmatrix}\begin{bmatrix}u_1\\ u_2\end{bmatrix}$$

$$\begin{bmatrix}y_1\\ y_2\end{bmatrix} = \begin{bmatrix}2.032 & -0.3439\\ -1.389 & 0.2208\end{bmatrix}\begin{bmatrix}x_1\\ x_2\end{bmatrix} + \begin{bmatrix}0 & 0\\ 0 & 0\end{bmatrix}\begin{bmatrix}u_1\\ u_2\end{bmatrix}$$

since they accurately capture the system's internal states and genuine dynamics. In comparison to other classic mathematical models, state-space models offer the advantages of simple control configuration and high precision in fast, complex, and MIMO-based dynamic processes.[47] Additionally, state-space models are widely used in MIMO systems.[48]

Various models using both the prediction focus and simulation focus with the PEM estimation method have been developed using various iterative search options such as Gauss−Newton, trust-region reflective Newton (lsqnonlin), gradient search (grad), and so forth. In both the prediction and simulation focus models, the second-order continuous-time state-space models give the highest fitting percentages for both Y_1 and Y_2. The fitting percentage is the key factor that illustrates how much the identified model is similar to the real plant behavior.[49] The identified models along with the identification procedure and fitting percentages are shown in Table 4.

As detailed in Table 4, the highest fitting percentage is shown by SS 3 (model 1) and SS 6 (model 2) models, which are based on prediction and simulation focus, respectively. Both the models are based on the PEM estimation method with trust-region reflective Newton (lsqnonlin) iteration search method.

Figure 8 illustrates the output responses for different identified state-space models. The term "plant output" refers to data generated from the Aspen Dynamics simulation of the pilot scale CO_2 capture plant, whereas "predicted/simulated output" refers to the output predicted by the state-space model identified in the System Identification Toolbox using the prediction and simulation focus with the PEM estimation method. Figure 9a,b shows the prediction performance in comparison to the actual plant data of model 1 for both Y_1 and Y_2, respectively. The same procedure is repeated for model 2, and the resulting performances are illustrated in Figure 10a,b. The actual range of the Y_1 output is 0.3326 to 0.3453 kmol/kmol and for the Y_2 output is 101.95 to 105.19 °C. However, the data are processed by removing means and scaled (range of −1 to 1) to ensure that the identification process should consider all the data equally through minimizing the range difference of data signals.[35]

The general equations for the state-space models are shown in eqs 9 and 10. In the equations, *A*, *B*, *C*, and *D* are the coefficient matrices as follows:

A = state or the system matrix
B = input matrix
C = output matrix
D = feedthrough matrix
u_1, u_2 = inputs or manipulated variables (MVs)
y_1, y_2 = outputs or controlled variables (CVs)
x_1, x_2 = states of the system

The values for *A*, *B*, *C*, and *D* are identified using the above-mentioned system identification process, and the final state-space equations of both models are illustrated in Table 5. The

https://doi.org/10.1021/acsomega.1c05974
ACS Omega 2022, 7, 8437−8455

gain or the feedthrough matrix (D) is zero as the system does not have direct feedthrough. The gain matrix of the observer, which is used for the Fast MPC, is designed based on pole locations. Therefore, the model is identified such that the feedthrough matrix has zero value initially.

3.3. Fast MPC Results. After the models have been checked for stability, controllability, and observability, the Fast MPC controller is then implemented using the 2 × 2 state-space models in MATLAB with a running time of 200 s. The 2 × 2 system refers to a system having two MVs and two CVs. In this control scheme, U_1 and U_2 are MVs, while Y_1 and Y_2 are CVs. In any control scheme, the control objective is to reject the disturbances and keep the CVs according to the given setpoints.[50] The models identified in Section 2.2 are developed using a large number of input−output data points. Therefore, these models are expected to perform well within the operating conditions covered in the identification stage. However, if the operating points of the plant are changed drastically, the models have to be reidentified as it is normally done even for standard MPC or in the presence of a common control loop malfunction, as valve stiction.[51−53]

To analyze the effectiveness of the identified models 1 and 2 on the performance of Fast MPC, the controller performance is evaluated by introducing step changes of ±5% in Y_1 and ±15% in Y_2, respectively. The higher step changes in the CO_2 composition of sweet gas are not practically observed during the plant operation.[33] The energy requirement for the regeneration step may fluctuate significantly, especially in the post-combustion CO_2 capture plant, as the power demands may vary during peak hours. As a result, the reboiler heat duty is also changed with high amplitudes.[54]

As the CO_2 absorption/stripping system is highly integrated, a change in one part of the plant affects the rest of the system as well due to the process interaction. Hence, when a step change is introduced in the output variable Y_1, the output variable Y_2 is also disturbed from its nominal value. Similarly, when a step change is introduced in the output Y_2, the output Y_1 is also being disturbed. Hence, both setpoint and disturbance changes can be observed simultaneously in this integrated system. As shown in the subsequent sections, the controller can reject the disturbance and achieve the nominal value with negligible offsets. Similar behavior has been observed for step changes in the output variable Y_2.

3.3.1. Step Change of ±5% in the Setpoint of the Output Variable Y_1. First, a step change of ±5% has been introduced at 60 s in Y_1 as higher step changes in the CO_2 composition of sweet gas or the top outlet gas of the absorber in absorption/stripping systems are not practically observed.[33] As described in Table 6, Fast MPC 1 utilizes model 1 (prediction focus model), whereas Fast MPC 2 adopted model 2 (simulation focus model) in determining the optimal input moves and output responses.

Figure 11a,b shows the responses of Y_1 and U_1 for both controllers described in Table 6 when there is a step change of +5% in Y_1. The Q and R matrices play an important role in the perfect tuning of the Fast MPC controllers in terms of overshoot and offsets.[55] The CO_2 composition in the sweet gas (Y_1) of the absorber is inversely proportional to the lean solvent valve opening (U_1). The lower lean solvent amount results in a lower amount of CO_2 absorbed in the MEA solvent, resulting in a higher amount of CO_2 present in the sweet gas stream. Therefore, when the controller is set to +5% step change in Y_1, U_1 is decreased to increase the Y_1 value.

Table 6. Fast MPC Controller Implementation

controller	dynamic model used
Fast MPC 1	model 1 = SS 3 (prediction focus based)
Fast MPC 2	model 2 = SS 6 (simulation focus based)

The objective of any controller is to rapidly reach the new setpoint in order to ensure optimal performance when the system is subjected to such abrupt change. Based on the results shown in Figure 11, the performance of the Fast MPC 1 controller is better than Fast MPC 2. The controller can achieve the desired new setpoint value of 0.1 precisely with the negligible offset for the prediction focus model case. However, the Fast MPC 2 controller, which is based on the simulation focus model, results in an offset of 0.002.

In addition, as the step change is introduced only in the output variable Y_1, the output variable Y_2 should be maintained at the original steady-state (nominal value of 0 in the scaled range) after the sudden disturbance. Figure 12a,b shows the responses of both Y_2 and U_2. As shown in Figures 12a and 14a, Y_2 has a higher offset for the Fast MPC 2 compared to the Fast MPC 1. As described in Section 2.4, the offset removal function is not incorporated within the mathematical eqs 5, 7 and 8 of the Fast MPC control algorithm. The Fast MPC solves the fragmental QP through state variables instead of output errors like standard MPC.[18] Moreover, the Fast MPC is an approximation method, which solves the optimization problem through exploited mathematical equations.[39] Therefore, offsets are present in the outputs, and the accuracy of the optimal solution is compromised to a negligible extent with the advantage of fast output responses. Based on these results, it can be concluded that the Fast MPC 1 controller, which is based on the prediction focus model, has negligible offsets in the setpoints of both Y_1 and Y_2. Figure 12a illustrates that the fluctuation and offset in the Fast MPC 2 are higher compared to Fast MPC 1. These results clearly exhibit the importance of selecting the appropriate dynamic model in ensuring the optimal performance of any model-based controller such as Fast MPC.

In the simulation results, R and Q are the weights for the input and state variables, respectively. By appropriate tunning of weights, the performance of any control strategy can be improved significantly. The R and Q matrices indicate the relative relevance of error minimization and control effort minimization from sample to sample during simulation.[56] Weights are tuned in MPC-based control schemes to successfully attain the required setpoints. The values of Q and R cannot be identical for all control strategies as each controller strategy's weights are tuned for the maximum performance.[57] Fast MPC 1 and 2 are based on two distinct models in the current study. As a result, each Fast MPC must have unique tuning parameters that optimize performance while minimizing offsets and errors. Additionally, decreasing Q and increasing R can eliminate offsets in output responses. As can be seen, the Fast MPC 2 is based on a Q value of [0.0002 0.0002], which is significantly less than the Fast MPC 1. However, Fast MPC 1 still performs better than Fast MPC 2.

Figure 13 and 14 show the responses of Y_1, U_1, Y_2, and U_2 for −5% step change in Y_1 for Fast MPC based on both models. The overall response patterns for CVs and MVs for −5% step change are similar to the +5% step change discussed previously. The overall results illustrate that the Fast MPC 1

https://doi.org/10.1021/acsomega.1c05974
ACS Omega 2022, 7, 8437−8455

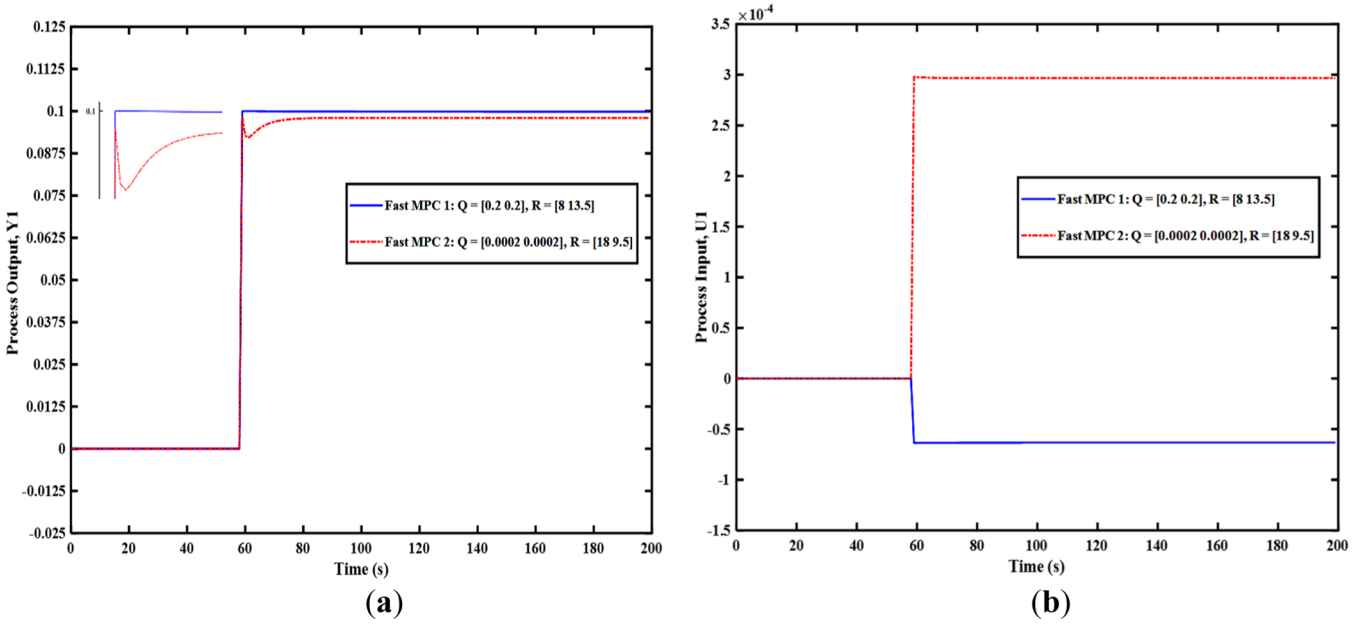

Figure 11. Setpoint tracking responses of Fast MPC 1 and 2 for +5% step change in Y_1: (a) output Y_1 and (b) input U_1.

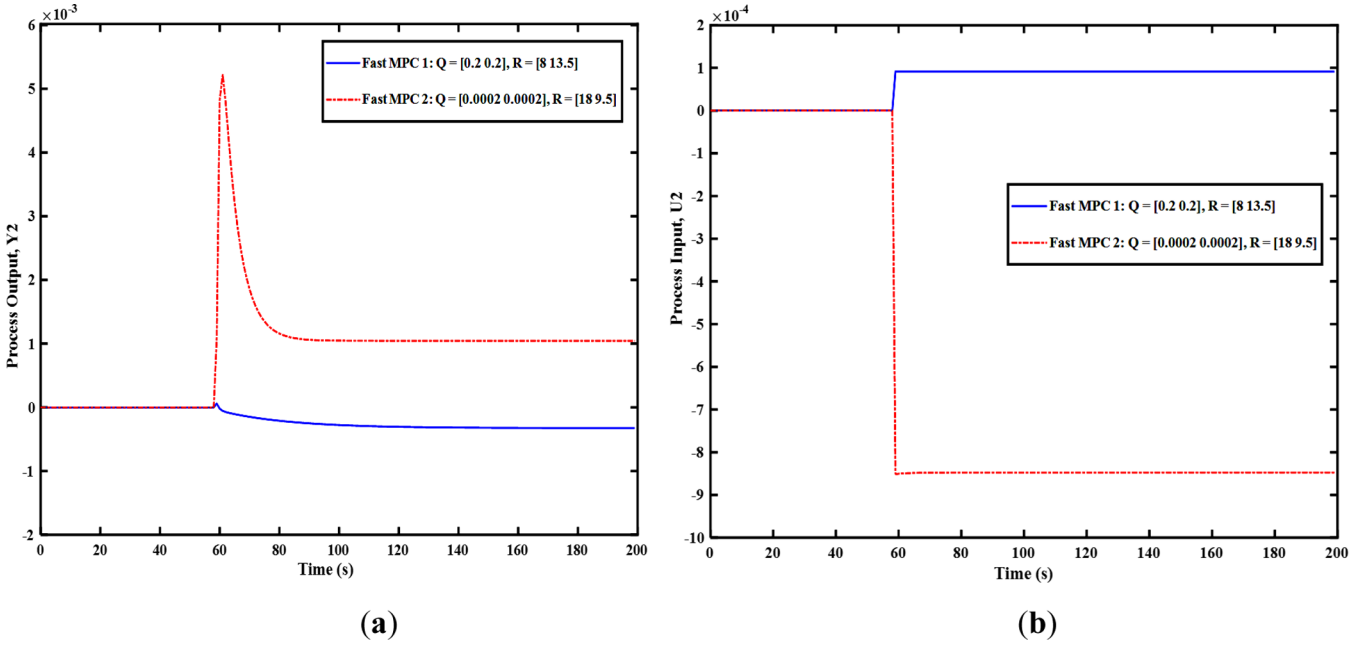

Figure 12. Setpoint tracking responses of Fast MPC 1 and 2 for +5% step change in Y_1: (a) output Y_2 and (b) input U_2.

controller has superior performance in terms of setpoint tracking with minimum overshoot and offsets as compared to the controller using the simulation focus model.

3.3.2. Controller Performance Parameters for ±5% Step Change. The typical criteria normally reported for the controller performance are the offset, settling time, and IAE and ISE values based on the differences between the desired setpoints and the actual outputs obtained.[13,58] The values for these four performance parameters have been calculated for ±5% step changes in Y_1. Table 7 shows the settling time and offset values for ±5% step change in Y_1 for both controllers. For +5% step change, the settling times for Y_1 and Y_2 for Fast MPC 2 are 29 and 38 s, while the values are 36 and 57 s for the Fast MPC 1 controller, respectively. The slightly larger settling time for the Fast MPC 1 may be due to the slower settling response because of the one-step ahead prediction behavior of the model.

However, the Fast MPC 1 controller has much better performance in terms of offsets, with 19.8% less offset value for Y_1 as compared to the Fast MPC 2. Similarly, the offset is 0.0007 higher for the Fast MPC 2 for Y_2 as compared to the Fast MPC 1. Additionally, the IAE value for the Fast MPC 2 is also much higher for +5% step change in Y_1, as shown in Table 7. Similar behavior has been observed for −5% step change in Y_1. In terms of ISE values, the Fast MPC 2 controller performance results in the output error value of approximately 0.0008, which is 200 times higher than Fast MPC 1. Based on these performance parameter results, it can be concluded that

https://doi.org/10.1021/acsomega.1c05974
ACS Omega 2022, 7, 8437−8455

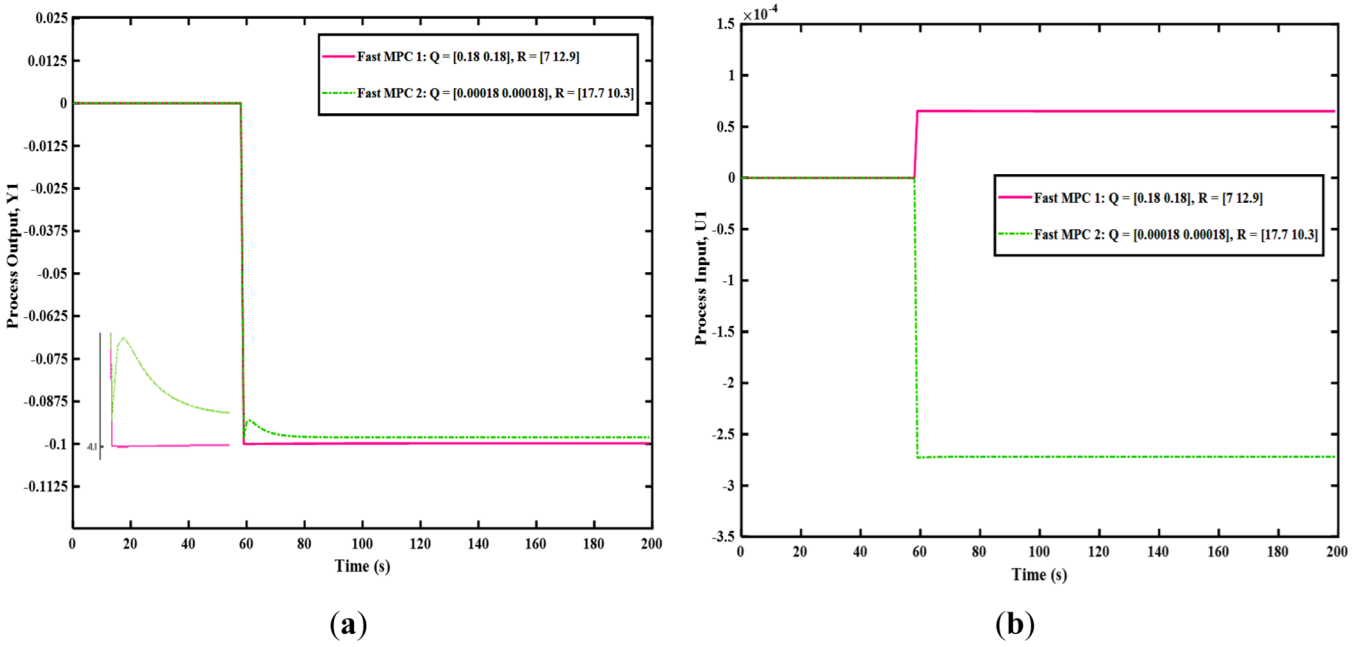

Figure 13. Setpoint tracking responses of Fast MPC 1 and 2 for −5% step change in Y_1: (a) output Y_1 and (b) input U_1.

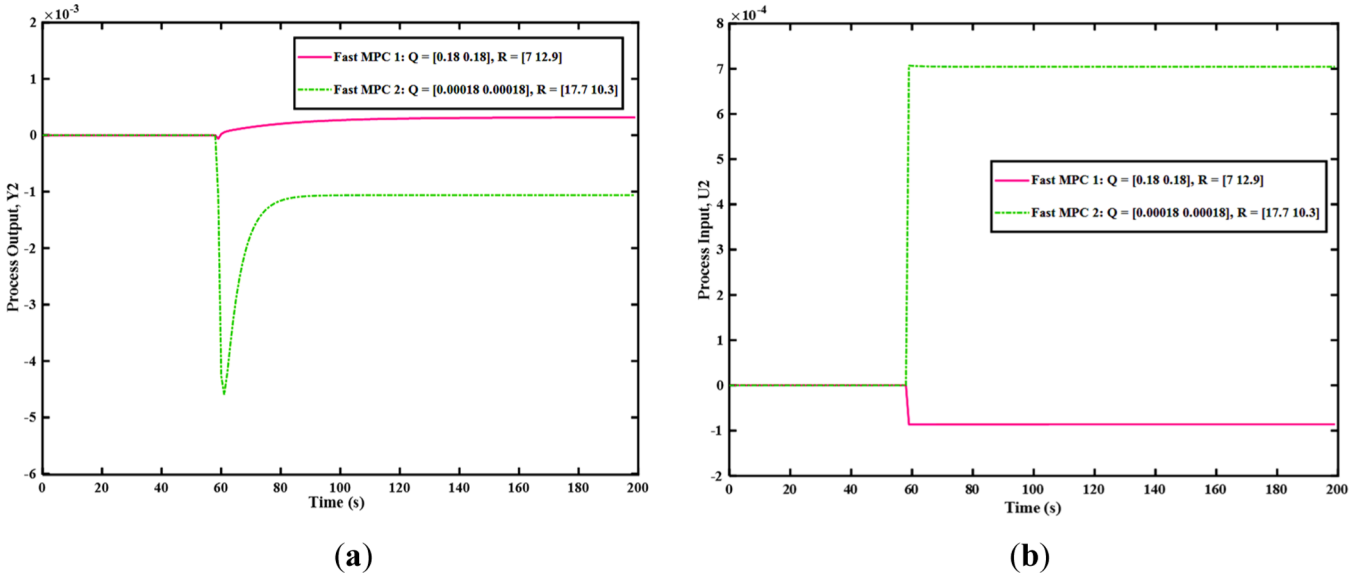

Figure 14. Setpoint tracking responses of Fast MPC 1 and 2 for −5% step change in Y_1: (a) output Y_2 and (b) input U_2.

Table 7. Controller Performance Parameters for ±5% Step Change in Y_1

		settling time (s)		offset			
step changes in Y_1 (%)	controller type	Y_1	Y_2	Y_1	Y_2	IAE	ISE
+5	Fast MPC 1	36	57	0.0002	0.0003	0.0226	0.000003
	Fast MPC 2	29	38	0.002	0.0010	0.3240	0.0008
−5	Fast MPC 1	40	67	0.0002	0.0003	0.0216	0.000003
	Fast MPC 2	24	22	0.002	0.0011	0.3116	0.0007

the Fast MPC controller has better performance in terms of offsets, IAE, and ISE when it is implemented using the prediction focus state-space models. The marginally slower response in terms of settling time can be balanced by the lower values of the other key performance parameters such as offsets, IAEs, and ISEs.

The accuracy of the identified model plays a major role in the evaluation of the overall computational time of the controller. The CPU time increases with the increase in states or variables of an identified mathematical model. The CPU time for the Fast MPC 1 and 2 controllers have been calculated in the MATLAB using Intel Core i7-10510U CPU@1.80 GHz, 2304 MHz processor. The Fast MPC control algorithm is

https://doi.org/10.1021/acsomega.1c05974
ACS Omega 2022, 7, 8437−8455

operated for 10 runs, and CPU time for each step change is calculated. The CPU time values for each step change for the Fast MPC 1 and 2 are shown in Table 8. The average CPU time for ±5% step change for the Fast MPC 2 is 11.22 s, while for the Fast MPC 1, it is 10.88 s. It can be concluded that the CPU time for both controllers is comparatively similar with negligible difference.

Table 8. CPU Time Values for ±5% Step Change in Y_1

controller type	step changes in Y_1 (%)	CPU time (s)	average (s)
Fast MPC 1	+5	11.47	10.88
	−5	10.3	
Fast MPC 2	+5	11.65	11.22
	−5	10.8	

3.3.3. Step Change of ±15% in the Setpoint of the Output Variable Y_2. The control strategy should be flexible enough to deal with such abrupt changes to maintain output variables at their setpoints.[58] Therefore, the Fast MPC control strategy performance is evaluated under a large step change of ±15% at 60 s in Y_2 as the stripper temperature fluctuates with high amplitude, a possible scenario during operation due to changing power plant energy requirements.[54] Figure 15 and 16 show the responses of Y_2, U_2, Y_1, and U_1 for Fast MPC 1 and 2 when there is a step change of +15% in Y_2. The stripper temperature (Y_2) is directly proportional to the reboiler heat duty (U_2). The controller maintains the new setpoint of Y_2 by changing the U_2 accordingly.

The Fast MPC is required to achieve the desired new setpoint value of 0.3 for Y_2. It can be observed that Fast MPC 1 controller is able to achieve the new setpoint successfully with negligible offsets. However, the Fast MPC 2 is not able to achieve the desired setpoint, resulting in an offset value of 0.0046. Moreover, the response of U_2 is opposite for the Fast MPC 2 control scheme. Ideally, the U_2 value should increase for +15% step change in Y_2. However, the U_2 value is decreasing with a large amplitude, as shown in Figure 15b. Although the simulation focus model has a satisfactory fitting percentage during the system identification stage, the inverse response of U_2 for the simulation focus model indicates that this model is not suitable for the Fast MPC control scheme. Figure 16a,b illustrates the responses of Y_1 and U_1 as the Y_1 value should achieve the nominal value of 0 after a sudden change in Y_2 at 60 s. The Fast MPC 1 controller has a negligible offset value, while the controller 2 has a significant offset of 0.0072 and high initial fluctuation.

Despite the fact that the Fast MPC controller provides fast output responses, the existence of offsets may lemmatize the performance in complicated dynamic systems such as absorption/stripping systems. As a result, the values of significant tuning parameters are tuned to decrease offsets to insignificant levels. On the other hand, input responses become aggressive with minute modifications to obtain the minimum offsets. As indicated in Figures 15 and 16, U_1 and U_2 respond aggressively to the point of being critical. However, the current research compares several state-space models for the application of a Fast MPC controller to a complicated CO_2 absorption/stripping system for fast computing. The FMPC controller has been optimized to reduce offsets to a negligible level that may be tolerated at the price of the controller's fast output responses and aggressive input changes.[59]

As previously stated, the weights (Q and R) can be modified to obtain desirable setpoints dependent on the magnitude of the step change.[10] The weights are always different for each control strategy, depending on the characteristics of the control algorithm and the nature of the model.[18] As a result, the weights for both Fast MPC 1 and 2 are tuned to yield setpoints with the minimum offsets and errors. A small value of Q and a large value of R is favorable for eliminating offsets and errors. The Q and R values of Fast MPC 2 are optimized to the maximum limits. However, the performance of Fast MPC 1 is still far better than the Fast MPC 2.

Similar behavior has been observed for −15% step change in Y_2. Figure 17a,b shows the responses of Y_2 and U_2. It can also be observed in Figure 18a that the Y_1 value is closer to 0 with

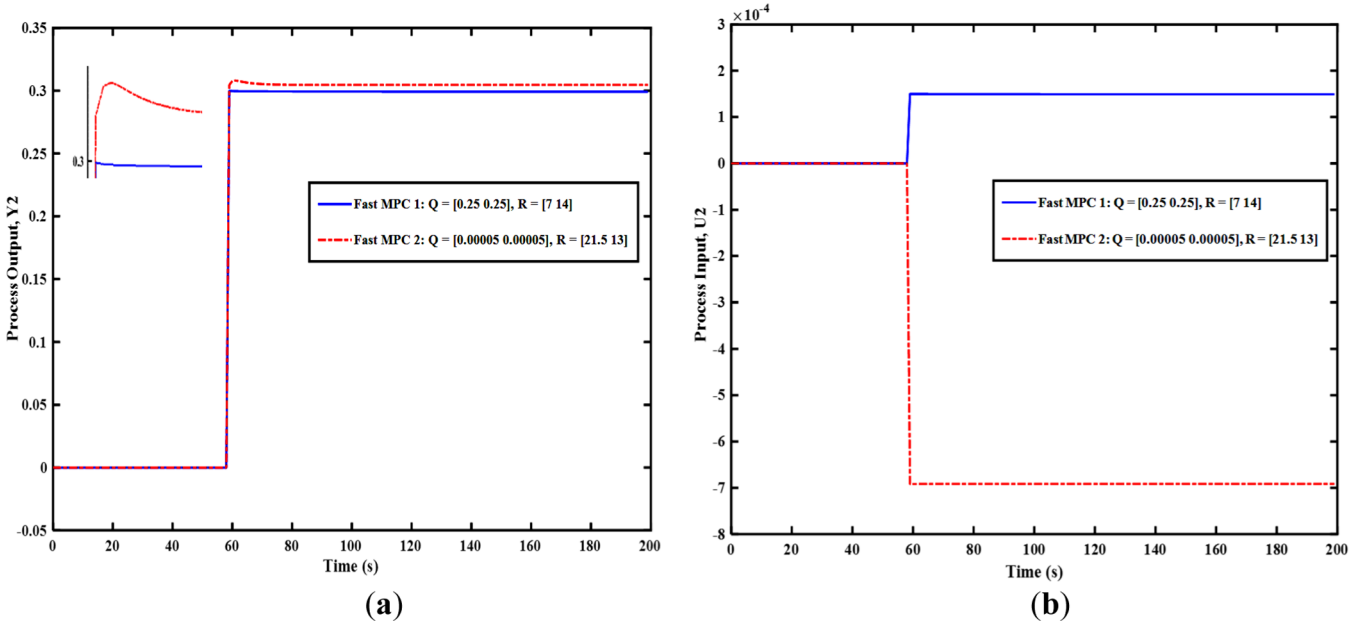

Figure 15. Setpoint tracking responses of Fast MPC 1 and 2 for +15% step change in Y_2 (a) output Y_2 (b) input U_2.

https://doi.org/10.1021/acsomega.1c05974
ACS Omega 2022, 7, 8437−8455

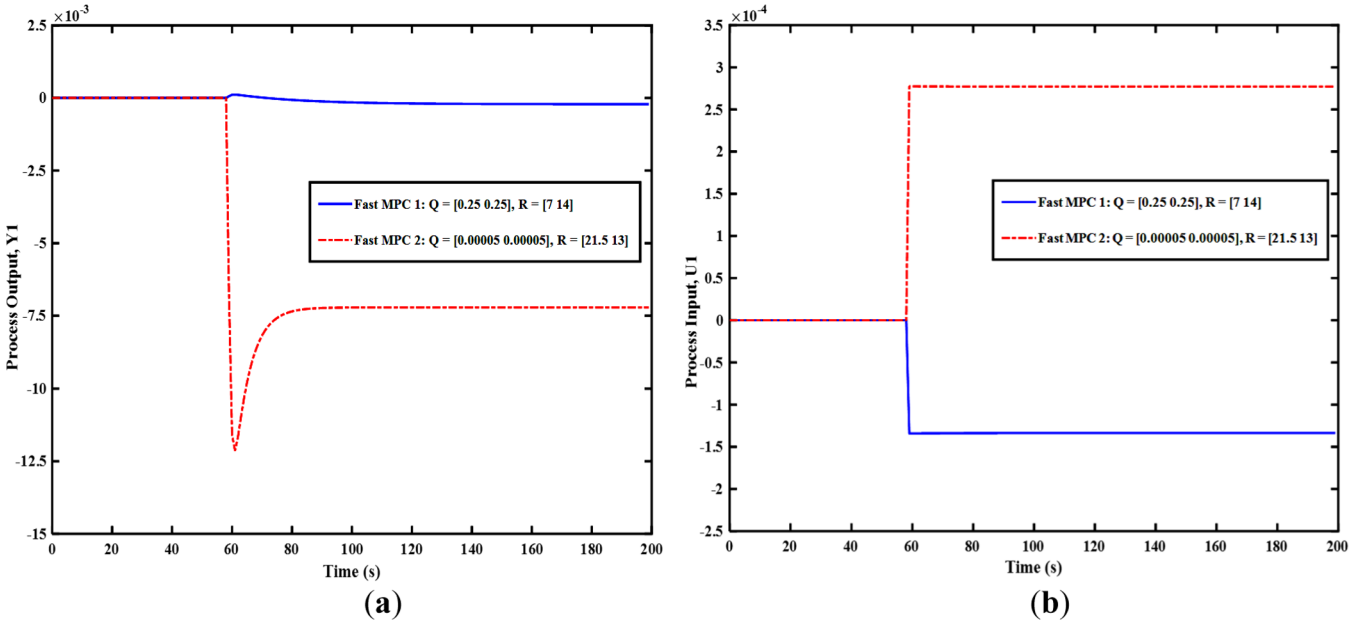

Figure 16. Setpoint tracking responses of Fast MPC 1 and 2 for +15% step change in Y_2: (a) output Y_1 and (b) input U_1.

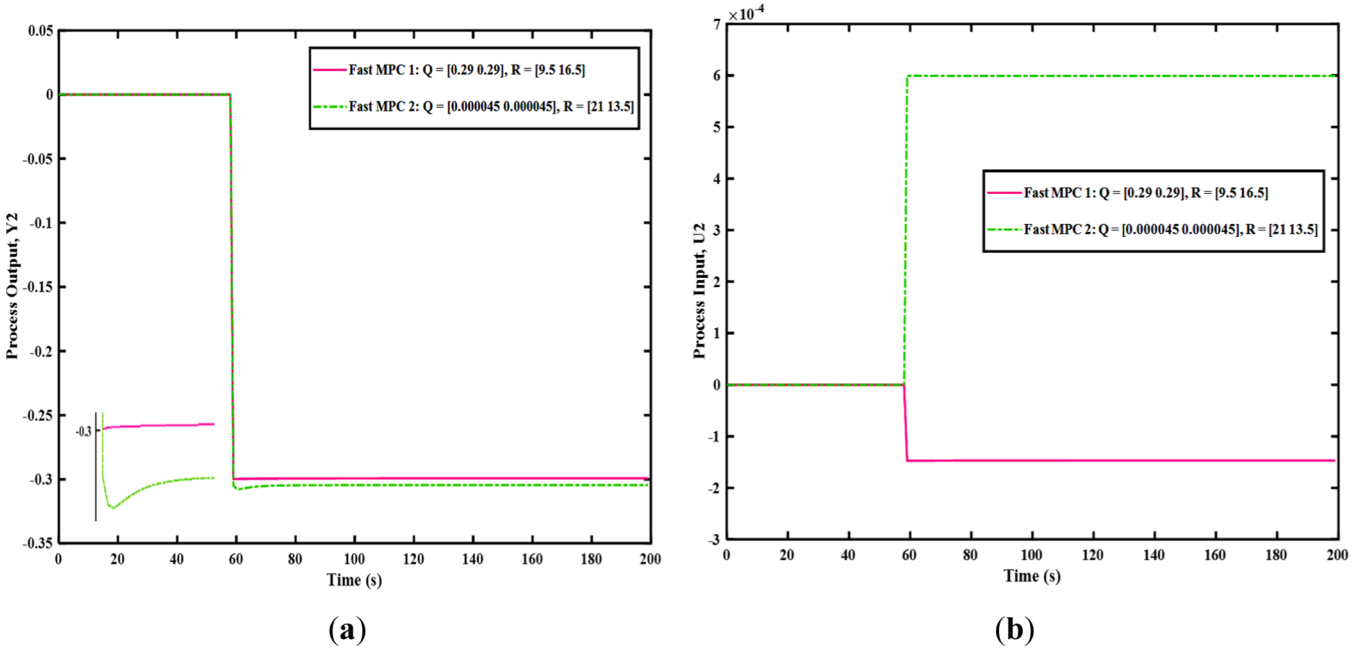

Figure 17. Setpoint tracking responses of Fast MPC 1 and 2 for −15% step change in Y_2: (a) output Y_2 and (b) input U_2.

negligible offsets for Fast MPC 1 controller compared to Fast MPC 2. Overall, the results for Fast MPC 1 are satisfactory with almost 0 offset for Y_1 and Y_2 as compared to the controller based on the simulation focus model.

3.3.4. Controller Performance Parameters for ±15% Step Change. The model comparison studies in terms of Fast MPC performance parameters have also been evaluated for a large step change of ±15% in Y_2. The overall result patterns are similar to the case, as described in Section 3.3.1. In Table 9, the settling time and offset are shown for ±15% step change in Y_2 for both the controllers. The settling time of the Fast MPC 2 in terms of Y_1 is 28 and 24 s for +15 and −15% step change in Y_2, respectively, while for the Fast MPC 1, the values for the same variables are 73 and 89 s. A similar pattern has been observed for the Y_2 variable as well. However, the Fast MPC 1 controller has superior performance in terms of offsets. The Fast MPC 2 controller results in an offset of 0.0046 for ±15% step change in Y_2, whereas the controller 1 has the offset value of just 0.0008. The offset is believed as the key parameter in terms of controller performance and accuracy.[60] Therefore, a lower offset for the Fast MPC 1 controller is a strong indicator that the prediction focus model is more suitable for the Fast MPC implementation on a CO_2 capture plant with the absorption/stripping system.

Moreover, the IAE and ISE values also indicate that the Fast MPC 1 has better performance for an effective and fast responsive control. Table 9 shows that the IAE value for the Fast MPC 2 is 6.24 and 6.63 times higher than the Fast MPC1

https://doi.org/10.1021/acsomega.1c05974
ACS Omega 2022, 7, 8437−8455

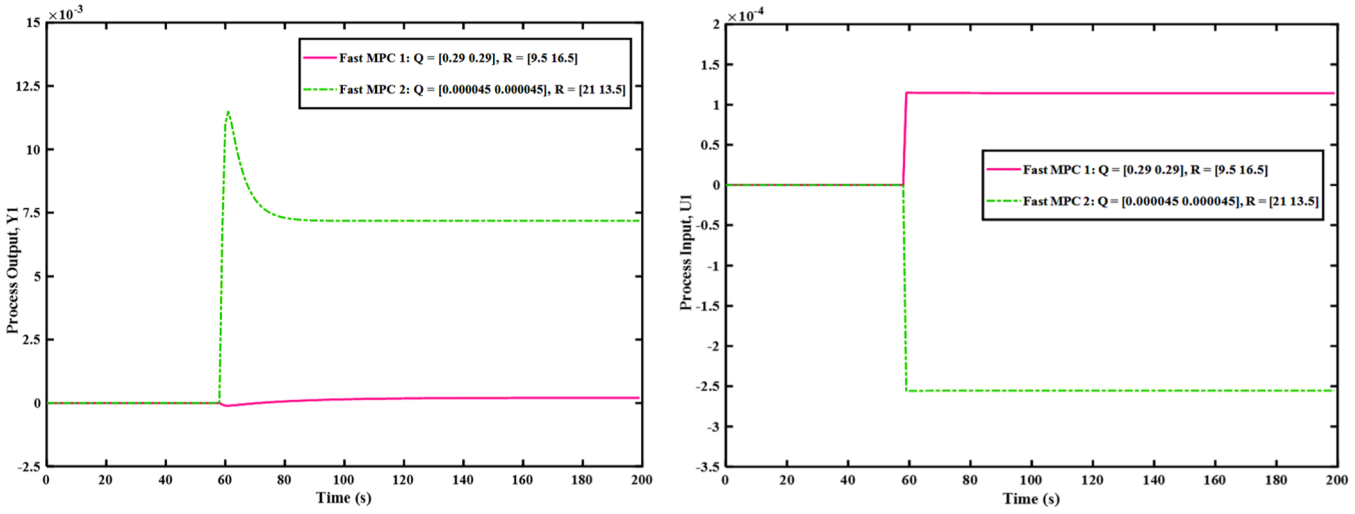

(a) (b)

Figure 18. Setpoint tracking responses of Fast MPC 1 and 2 for −15% step change in Y_2: (a) output Y_1 and (b) input U_1.

Table 9. Controller Performance Parameters for ±15% Step Change in Y_2

		settling time (s)		offset			
step changes in Y_2 (%)	controller type	Y_1	Y_2	Y_1	Y_2	IAE	ISE
+15	Fast MPC 1	73	39	0.0002	0.0008	0.1068	0.00008
	Fast MPC 2	28	22	0.0072	0.0046	0.6664	0.0032
−15	Fast MPC 1	89	55	0.0002	0.0008	0.1003	0.00007
	Fast MPC 2	24	22	0.0072	0.0046	0.6646	0.0032

based on prediction focus model, while the ISE values for the Fast MPC 2 are 4 and 4.58 times higher than the Fast MPC 1 for +15 and −15% step change, respectively. The results conclude that the Fast MPC 1 based on the prediction focus model has better performance for the CO_2 capture plant based on the absorption/stripping system. This superior performance might be due to a one-step ahead predictive nature that allows for the higher fitting percentage of the model as compared to the simulation focus model.

The CPU time of the Fast MPC control algorithm for ±15% step change in the setpoint of Y_2 output is calculated similarly, as described in Section 3.3.2. The average CPU time for ±15% step change for the Fast MPC 1 is 10.23 s, while for the Fast MPC 2, it is 11.89 s. The CPU time values for both controllers have been listed in Table 10. Based on the CPU time values, it

Table 10. CPU Time Values for ±15% Step Change in Y_2

controller type	step changes in Y_2 (%)	CPU time (s)	average (s)
Fast MPC 1	+15	10.63	10.23
	−15	9.83	
Fast MPC 2	+15	11.89	11.89
	−15	11.88	

can be concluded that Fast MPC controller based on the prediction focus state-space space model requires less time to solve the integrated structure or the control problem than the controller based on the simulation focus model.

3.3.5. Comparison of Fast MPC and Standard MPC. Once the appropriate model is evaluated through controller performance parameters in the above sections, the Fast MPC and the standard MPC controllers are implemented on model 1, and the results are compared. A step change of +5% is introduced in the setpoint of the output variable Y_1. For both controllers, Figure 19 depicts the response of Y_1 to +5% step change in Y_1. As illustrated, the Fast MPC controller reached the new setpoint value quickly with negligible offsets. The standard MPC controller, on the other hand, has a longer settling time than the Fast MPC, resulting in a prolonged setpoint attainment. According to the energy requirements, CO_2 capture facilities must operate at particular CO_2 capture rates. In actual applications, the slower settling time of outputs is undesirable since it can drastically reduce the crucial CO_2 capture rate. In addition, the setpoint of the Y_1 output in the case of the standard MPC controller has significantly large offsets.

The slower response time of the standard MPC controller might be related to the computational burden of the control algorithm's solution in the form of a sophisticated QP. The Y_2 output should be kept at its nominal value since the step change in the setpoint of the Y_1 output has just been employed. The value of Y_2 differs from the standard value as a result of the step change in Y_1, as seen in Figure 20. Nevertheless, both controllers can reject the disturbance and keep the Y_2 output at its nominal value. While the disturbance in the case of the Fast MPC controller is quite minimal, the standard MPC controller has a fairly substantial initial fluctuation. Ideally, outputs must match setpoints exactly since offsets have a significant influence on the performance of the designed control strategy.[61]

The required setpoints must be obtained with small offsets in any control strategy as offsets are critical parameter affecting the controller's performance and accuracy.[58,60] The settling time to achieve the new setpoints and IAE values are also an important aspect to estimate the performance of any control

https://doi.org/10.1021/acsomega.1c05974
ACS Omega 2022, 7, 8437−8455

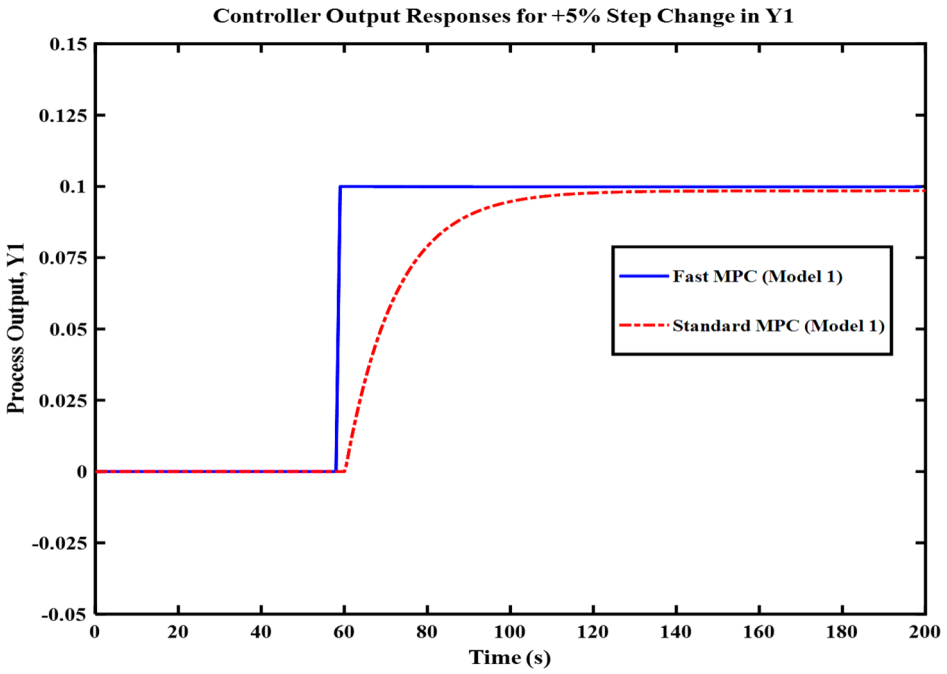

Figure 19. Output Y_1 response of Fast MPC and standard MPC for +5% step change.

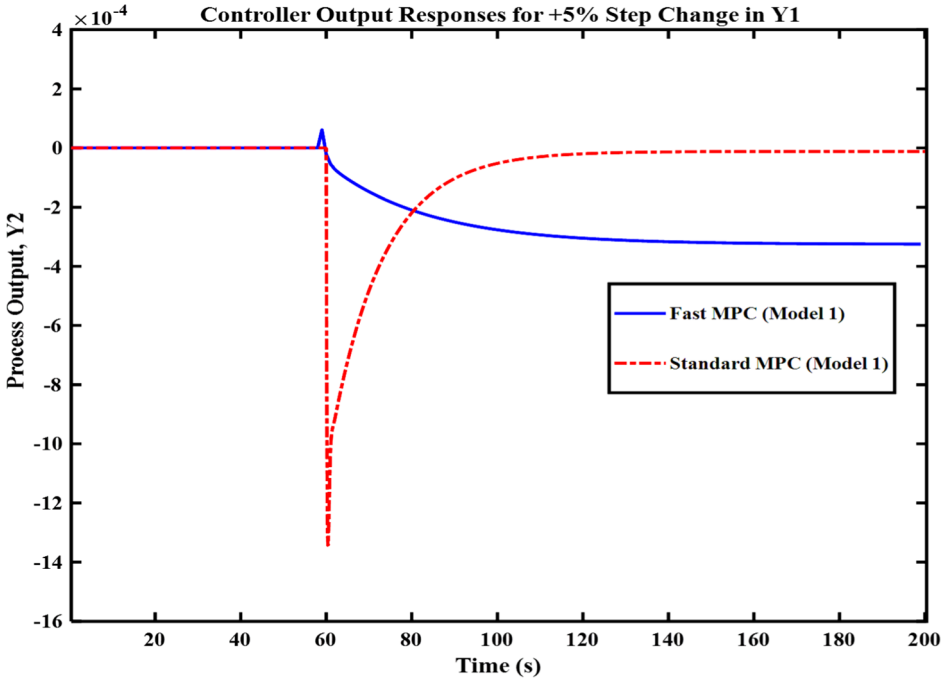

Figure 20. Output Y_2 response of Fast MPC and standard MPC for +5% step change.

scheme. For both controllers, the values of settling time and IAE error have been calculated. The Fast MPC controller is typically used in electronic systems when dynamic complexity is not a problem, and sampling times are measured in seconds. In the current study, the standard MPC controller has a settling time of 84 and 97 s for Y_1 and Y_2, respectively, whereas the Fast MPC controller has a settling time of 36 and 57 s. In terms of settling time, the Fast MPC controller appears to outperform the standard MPC. The offset for both controllers is maintained to a minimum due to the emphasis on fast response time and low error values. The standard MPC has 1.4913 IAE values, whereas the Fast MPC has 0.0226, suggesting that the Fast MPC controller is a better choice than the standard MPC to achieve the setpoint quickly with minimum errors.

4. CONCLUSIONS

The purpose of this paper is to investigate the possible implementation of the Fast MPC controller scheme for chemical systems. Due to the difficulties associated with complicated dynamic behavior and model sensitivity, which results in considerable offsets, the Fast MPC controller has not been implemented on the CO_2 capture plant based on the absorption/stripping system. The main objective of this work

https://doi.org/10.1021/acsomega.1c05974
ACS Omega 2022, 7, 8437−8455

is to evaluate the most appropriate state-space model for implementing the Fast MPC control strategy, which results in fast output responses, negligible offsets, and minimum errors. The results showed that the Fast MPC based on the state-space prediction focus model (Fast MPC 1 controller) has on average of 7.9 times lower offset than the simulation focus model and 10.4 times lower IAE values. The computational efficiency in terms of CPU time for both models has been calculated. The Fast MPC based on the prediction focus model has the gross mean CPU time of 10.55 s, while the Fast MPC based on the simulation focus model has the value of 11.55 s. The comparison study concluded that the Fast MPC control strategy performs efficiently using the prediction-based focus state-space model (model 1) for CO_2 capture plant using absorption/stripping systems with minimum offsets and errors. Furthermore, the comparison of the Fast MPC controller based on model 1 with the standard MPC also revealed the effectiveness of the Fast MPC control strategy. The related future works include (1) evaluating the Fast MPC performances in ramp changes or diurnal oscillation scenarios, (2) the possibility of expanding the Fast MPC strategy to include other variables in the CO_2 absorption/stripping system, and (3) to investigate the possibility of reformulating the algorithm to eliminate the offsets.

AUTHOR INFORMATION

Corresponding Author

Haslinda Zabiri − *Chemical Engineering Department, Universiti Teknologi PETRONAS, 32610 Bandar Seri Iskandar, Perak, Malaysia;* orcid.org/0000-0003-1821-1028; Phone: +6053687625; Email: haslindazabiri@utp.edu.my; Fax: +6053656176

Authors

Tahir Sultan − *Chemical Engineering Department, Universiti Teknologi PETRONAS, 32610 Bandar Seri Iskandar, Perak, Malaysia;* orcid.org/0000-0002-1448-9279

Muhammad Shahbaz − *Division of Sustainable Development, College of Science and Engineering, Hamad Bin Khalifa University, 5825 Doha, Qatar;* orcid.org/0000-0003-2295-8167

Abdulhalim Shah Maulud − *Chemical Engineering Department, Universiti Teknologi PETRONAS, 32610 Bandar Seri Iskandar, Perak, Malaysia;* orcid.org/0000-0002-3590-7492

Complete contact information is available at: https://pubs.acs.org/10.1021/acsomega.1c05974

Notes

The authors declare no competing financial interest.

ACKNOWLEDGMENTS

The authors like to express their appreciation to the Ministry of Higher Education (MOHE), grant reference code FRGS/1/2018/TK02/UTP/02/5 for the funding provided for this research. The authors would also like to extend their appreciation to Yayasan Universiti Teknologi PETRONAS (YUTP) (grant 015LC0-139) for additional funding provided for this work.

REFERENCES

(1) Alcheikhhamdon, Y.; Hoorfar, M. Natural gas quality enhancement: A review of the conventional treatment processes, and the industrial challenges facing emerging technologies. *J. Nat. Gas Sci. Eng.* **2016**, *34*, 689−701.

(2) Sanni, S. E.; Agboola, O.; Fagbiele, O.; Yusuf, E. O.; Emetere, M. E. Optimization of natural gas treatment for the removal of CO2 and H2S in a novel alkaline-DEA hybrid scrubber. *Egypt. J. Pet.* **2020**, *29*, 83−94.

(3) Vente, J. F.; Haije, W. G. Emerging Opportunities for Natural Gas Treatment and CO2 Capture. *Proceedings of the 4th International Gas Processing Symposium*, 2015; pp 133−139.

(4) Wu, X.; Wang, M.; Liao, P.; Shen, J.; Li, Y. Solvent-based post-combustion CO2 capture for power plants: A critical review and perspective on dynamic modelling, system identification, process control and flexible operation. *Appl. Energy* **2020**, *257*, 113941.

(5) Lee, S.-Y.; Park, S.-J. A review on solid adsorbents for carbon dioxide capture. *J. Ind. Eng. Chem.* **2015**, *23*, 1−11.

(6) Global CCS Institute. The Global Status of CCS, 2018. https://www.globalccsinstitute.com/resources/global-status-report/previous-reports/ (March 01).

(7) United Nations Climate Change. Historic Paris Agreement on Climate Change. https://unfccc.int/process-and-meetings/the-paris-agreement/the-paris-agreement (March 01).

(8) Rufford, T. E.; Smart, S.; Watson, G. C. Y.; Graham, B. F.; Boxall, J.; Diniz da Costa, J. C.; May, E. F. The removal of CO2 and N2 from natural gas: A review of conventional and emerging process technologies. *J. Pet. Sci. Eng.* **2012**, *94*−*95*, 123−154.

(9) Qasim, M.; Ayoub, M.; Aqsha, A.; Zulfiqar, M. Preparation of Metal Oxide-based Oxygen Carriers Supported with CeO 2 and γ -Al 2 O 3 for Chemical Looping Combustion. *Chem. Eng. Technol.* **2021**, *44*, 782−787.

(10) Hossein Sahraei, M.; Ricardez-Sandoval, L. A. Controllability and optimal scheduling of a CO 2 capture plant using model predictive control. *Int. J. Greenhouse Gas Control* **2014**, *30*, 58−71.

(11) Li, Z.; Ding, Z.; Wang, M.; Oko, E. Model-free adaptive control for MEA-based post-combustion carbon capture processes. *Fuel* **2018**, *224*, 637−643.

(12) Cormos, A.-M.; Vasile, M.; Cristea, M.-V., Flexible operation of CO2 capture processes integrated with power plant using advanced control techniques. *12th International Symposium on Process Systems Engineering and 25th European Symposium on Computer Aided Process Engineering,Computer Aided Chemical Engineering*, 2015; Vol. *37*, pp 1547-1552.

(13) He, X.; Lima, F. V. Development and implementation of advanced control strategies for power plant cycling with carbon capture. *Comput. Chem. Eng.* **2019**, *121*, 497−509.

(14) He, X.; Wang, Y.; Bhattacharyya, D.; Lima, F. V.; Turton, R. Dynamic modeling and advanced control of post-combustion CO2 capture plants. *Chem. Eng. Res. Des.* **2018**, *131*, 430−439.

(15) Luu, M. T.; Abdul Manaf, N.; Abbas, A. Dynamic modelling and control strategies for flexible operation of amine-based post-combustion CO2 capture systems. *Int. J. Greenhouse Gas Control* **2015**, *39*, 377−389.

(16) Rúa, J.; Hillestad, M.; Nord, L. O. Model predictive control for combined cycles integrated with CO2 capture plants. *Comput. Chem. Eng.* **2021**, *146*, 107217.

(17) Zhang, Q.; Turton, R.; Bhattacharyya, D. Development of Model and Model Predictive Control of a MEA-based Post-Combustion CO2 Capture Process. *Ind. Eng. Chem. Res.* **2016**, *55*, 1292−1308.

(18) He, Z.; Sahraei, M. H.; Ricardez-Sandoval, L. A. Flexible operation and simultaneous scheduling and control of a CO2 capture plant using model predictive control. *Int. J. Greenhouse Gas Control* **2016**, *48*, 300−311.

(19) Wu, X.; Shen, J.; Wang, M.; Lee, K. Y. Intelligent predictive control of large-scale solvent-based CO2 capture plant using artificial neural network and particle swarm optimization. *Energy* **2020**, *196*, 117070.

(20) Wu, X.; Shen, J.; Li, Y.; Wang, M.; Lawal, A.; Lee, K. Y. Nonlinear dynamic analysis and control design of a solvent-based

post-combustion CO2 capture process. *Comput. Chem. Eng.* **2018**, *115*, 397−406.
(21) Park, B. J.; Kim, Y.; Lee, J. M. Design of switching multilinear model predictive control using gap metric. *Comput. Chem. Eng.* **2021**, *150*, 107317.
(22) Cisneros, P. G.; Werner, H. Fast Nonlinear MPC for Reference Tracking Subject to Nonlinear Constraints via Quasi-LPV Representations. *IFAC-PapersOnLine* **2017**, *50*, 11601−11606.
(23) Quirynen, R.; Gros, S.; Diehl, M. Inexact Newton based Lifted Implicit Integrators for fast Nonlinear MPC**This research was supported by Research Council KUL: PFV/10/002 Optimization in Engineering Center OPTEC; Eurostars SMART; Belgian Federal Science Policy Office: IUAP P7 (DYSCO, Dynamical systems, control and optimization, 2012-2017); EU: FP7-TEMPO (MCITN-607957), ERC HIGHWIND (259166), H2020-ITN AWESCO (642682). R. Quirynen holds a PhD fellowship of the Research Foundation - Flanders (FWO). *IFAC-PapersOnLine* **2015**, *48*, 32−38.
(24) Schindele, D.; Aschemann, H. Fast Nonlinear MPC for an Overhead Travelling Crane. *IFAC Proceed. Vol.* **2011**, *44*, 7963−7968.
(25) Fonseca, I. M.; Bainum, P. M.; Santos, M. C. CPU time consideration for LSS structural/control optimization models with different degrees of freedom. *Acta Astronaut.* **2004**, *54*, 259−266.
(26) Warudkar, S. S.; Cox, K. R.; Wong, M. S.; Hirasaki, G. J. Influence of stripper operating parameters on the performance of amine absorption systems for post-combustion carbon capture: Part II. Vacuum strippers. *Int. J. Greenhouse Gas Control* **2013**, *16*, 351−360.
(27) George, E. C.; Riverol, C. Effectiveness of Amine Concentration and Circulation Rate in the CO2 Removal Process. *Chem. Eng. Technol.* **2020**, *43*, 942−949.
(28) Salvinder, K. M. S.; Zabiri, H.; Isa, F.; Taqvi, S. A.; Roslan, M. A. H.; Shariff, A. M. Dynamic modelling, simulation and basic control of CO2 absorption based on high pressure pilot plant for natural gas treatment. *Int. J. Greenhouse Gas Control* **2018**, *70*, 164−177.
(29) Bui, M.; Gunawan, I.; Verheyen, V.; Feron, P.; Meuleman, E.; Adeloju, S. Dynamic modelling and optimisation of flexible operation in post-combustion CO2 capture plants-A review. *Comput. Chem. Eng.* **2014**, *61*, 245−265.
(30) Dai, B.; Wu, X.; Liang, X.; Shen, J. Model predictive control of post-combustion CO2 capture system for coal-fired power plants. *2017 36th Chinese Control Conference (CCC)*; IEEE, 2017; pp 9315−9320.
(31) He, Z.; Ricardez-Sandoval, L. A. Dynamic modelling of a commercial-scale CO 2 capture plant integrated with a natural gas combined cycle (NGCC) power plant. *Int. J. Greenhouse Gas Control* **2016**, *55*, 23−35.
(32) MacDowell, N.; Florin, N.; Buchard, A.; Hallett, J.; Galindo, A.; Jackson, G.; Adjiman, C. S.; Williams, C. K.; Shah, N.; Fennell, P. An overview of CO2 capture technologies. *Energy Environ. Sci.* **2010**, *3*, 1645−1669.
(33) Sultan, T.; Zabiri, H.; Ali Ammar Taqvi, S.; Shahbaz, M. Plant-wide MPC control scheme for CO2 absorption/stripping system. *Mater. Today: Proc.* **2021**, *42*, 191−200.
(34) Hauger, S. O.; Flø, N. E.; Kvamsdal, H.; Gjertsen, F.; Mejdell, T.; Hillestad, M. Demonstration of non-linear model predictive control of post-combustion CO2 capture processes. *Comput. Chem. Eng.* **2019**, *123*, 184−195.
(35) Liao, P.; Wu, X.; Li, Y.; Wang, M.; Shen, J.; Lawal, A.; Xu, C. Application of piece-wise linear system identification to solvent-based post-combustion carbon capture. *Fuel* **2018**, *234*, 526−537.
(36) The MathWorks. *Simulate and predict identified model output*. https://www.mathworks.com/help/ident/ug/definition-simulation-and-prediction.html?s_tid=srchtitle.
(37) Fatima, A.; Zabiri, H.; Taqvi, S. A. A.; Ramli, N. System Identification of Industrial Debutanizer Column. *2019 9th IEEE International Conference on Control System, Computing and Engineering (ICCSCE)*; IEEE, 2019.
(38) Maruta, I.; Sugie, T. Stabilized Prediction Error Method for Closed-loop Identification of Unstable Systems. *IFAC-PapersOnLine* **2018**, *51*, 479−484.
(39) Wang, Y.; Boyd, S. Fast Model Predictive Control Using Online Optimization. *IFAC Proceed. Vol.* **2008**, *41*, 6974−6979.
(40) Nittaya, T.; Douglas, P. L.; Croiset, E.; Ricardez-Sandoval, L. A. Dynamic modelling and control of MEA absorption processes for CO2 capture from power plants. *Fuel* **2014**, *116*, 672−691.
(41) Gaspar, J.; Ricardez-Sandoval, L.; Jørgensen, J. B.; Fosbøl, P. L. Controllability and flexibility analysis of CO 2 post-combustion capture using piperazine and MEA. *Int. J. Greenhouse Gas Control* **2016**, *51*, 276−289.
(42) Knudsen, M. D.; Georges, L.; Skeie, K. S.; Petersen, S. Experimental test of a black-box economic model predictive control for residential space heating. *Appl. Energy* **2021**, *298*, 117227.
(43) Jamil, M.; Khan, M. N.; Rind, S. J.; Awais, Q.; Uzair, M. Neural network predictive control of vibrations in tall structure: An experimental controlled vision. *Comput. Electr. Eng.* **2021**, *89*, 106940.
(44) Armenise, G.; Vaccari, M.; Bacci di Capaci, R.; Pannocchia, G. An Open-Source System Identification Package for Multivariable Processes. *2018 UKACC 12th International Conference on Control (CONTROL)*; IEEE, 2018; pp 152−157.
(45) Garnier, H.; Gilson, M.; Laurain, V.; Ni, B. *Developments for the CONTSID toolbox*, 2012.
(46) Ninness, B.; Wills, A.; Mills, A. UNIT: A freely available system identification toolbox. *Control Eng. Pract.* **2013**, *21*, 631−644.
(47) Zhang, R.; Wu, S.; Gao, F. State Space Model Predictive Control for Advanced Process Operation: A Review of Recent Development, New Results, and Insight. *Ind. Eng. Chem. Res.* **2017**, *56*, 5360−5394.
(48) Van Mulders, A.; Schoukens, J.; Vanbeylen, L. Identification of systems with localised nonlinearity: From state-space to block-structured models. *Automatica* **2013**, *49*, 1392−1396.
(49) Gibanica, M.; Abrahamsson, T. J. S.; McKelvey, T. State-space system identification with physically motivated residual states and throughput rank constraint. *Mech. Syst. Signal Process.* **2020**, *142*, 106579.
(50) Salvinder, K. M. S.; Zabiri, H.; Taqvi, S. A.; Ramasamy, M.; Isa, F.; Rozali, N. E. M.; Suleman, H.; Maulud, A.; Shariff, A. M. An overview on control strategies for CO2 capture using absorption/stripping system. *Chem. Eng. Res. Des.* **2019**, *147*, 319−337.
(51) Chaves, C. R.; Rodrigo, J. C. G.; Garcia, C. Identification of the Dynamic Model of a Petrochemical Furnace of 50MW for Implementation of MPC Control. *IFAC-PapersOnLine* **2019**, *52*, 317−322.
(52) Wu, X.; Wang, M.; Liao, P.; Shen, J.; Li, Y. Solvent-based post-combustion CO2 capture for power plants: A critical review and perspective on dynamic modelling, system identification, process control and flexible operation. *Appl. Energy* **2020**, *257*, 113941.
(53) Bacci di Capaci, R.; Vaccari, M.; Scali, C.; Pannocchia, G. Enhancing MPC formulations by identification and estimation of valve stiction. *J. Process Control* **2019**, *81*, 31−39.
(54) Jung, H.; Im, D.; Heo, S.; Kim, B.; Lee, J. H. Dynamic analysis and linear model predictive control for operational flexibility of post-combustion CO2 capture processes. *Comput. Chem. Eng.* **2020**, *140*, 106968.
(55) Das, S.; Pan, I.; Halder, K.; Das, S.; Gupta, A. LQR based improved discrete PID controller design via optimum selection of weighting matrices using fractional order integral performance index. *Appl. Math. Model.* **2013**, *37*, 4253−4268.
(56) Mc Namara, P.; Negenborn, R. R.; De Schutter, B.; Lightbody, G. Weight optimisation for iterative distributed model predictive control applied to power networks. *Eng. Appl. Artif. Intell.* **2013**, *26*, 532−543.
(57) Cho, H.; Bacelli, G.; Coe, R. G. Model Predictive Control Tuning by Inverse Matching for a Wave Energy Converter. *Energies* **2019**, *12*, 4158.
(58) Wu, X.; Shen, J.; Li, Y.; Wang, M.; Lawal, A. Flexible operation of post-combustion solvent-based carbon capture for coal-fired power

https://doi.org/10.1021/acsomega.1c05974
ACS Omega 2022, 7, 8437−8455

plants using multi-model predictive control: A simulation study. *Fuel* **2018**, *220*, 931−941.
(59) Sultan, T.; Zabiri, H.; Shahbaz, M.; Maulud, A. S. Performance evaluation of the fast model predictive control scheme on a CO2 capture plant through absorption/stripping system. *Process Saf. Environ. Prot.* **2022**, *157*, 218−236.
(60) Huang, R.; Biegler, L. T.; Patwardhan, S. C. Fast Offset-Free Nonlinear Model Predictive Control Based on Moving Horizon Estimation. *Ind. Eng. Chem. Res.* **2010**, *49*, 7882−7890.
(61) Patron, G. D.; Ricardez-Sandoval, L. A robust nonlinear model predictive controller for a post-combustion CO2 capture absorber unit. *Fuel* **2020**, *265*, 116932.

https://doi.org/10.1021/acsomega.1c05974
ACS Omega 2022, 7, 8437−8455